Force Sensing Strategies for Robot-Assisted Minimally Invasive Surgery: A Review

Martijn Suurveld

March 9, 2021

Abstract

With the arrival of MIS, and subsequently RAMIS, surgeons have lost most of their force sensation during surgery. This has lead to more frequent slips, errors and tissue damage as well as an inability to palpate tissue. Therefore, the rise in popularity of MIS has resulted in a lot of literature being published on force sensing in MIS over the past 10 years.
This literature review provides an overview of the solutions that have been proposed to sense kinesthetic tip forces in MIS. The paper starts by identifying the applications of force sensing in MIS followed by the requirements associated with doing so. It shows that there are numerous and strict requirements, some of which only loosely defined and others conflicting. In the central part of this review the state-of-the-art was outlined and discussed at length. Analysis of the included literature revealed that there are still many aspects for which the field remains divided. In several instances this can be attributed to a lack of sufficiently representative validation. In this review it has become clear that trying to choose one sensing strategy over another is mostly a matter trade-offs between different requirements specific to each application.

Keywords: Force sensor, Force sensing, Force estimation, Kinesthetic forces, Force feedback, Minimally Invasive Surgery, Robot-assisted Minimally Invasive Surgery, Laparoscopy, Endoscopy.

1 Introduction

Over the past decades Minimally Invasive Surgery (MIS), also known as endoscopy or laparoscopy, has become the preferred approach to abdominal surgery. It is preferred because of the reduced invasiveness compared to conventional, open, surgery. Advantages of the reduced invasiveness include decreased tissue trauma, blood loss, post-operative pain and risk of infection as well as a shorter hospital stay. The surgery is performed with long slender instruments which are inserted into the inflated abdomen through small access ports. The access ports are fitted with a trocar to keep the abdomen inflated. An additional access port is required to pass the camera, called an endoscope, and gain vision inside the abdomen [1, 2].

Regardless of all the advantages that MIS offers it also has some limitations. Firstly, friction and backlash in the instrument, as well as the fulcrum effect caused by rotation around the access port, lead to a reduced and distorted force sensation. Experienced surgeons have learnt to cope with this distorted force sensation. They are able to extract some information about the tip forces through the images on the screen and the forces they still experience on the handle [3].

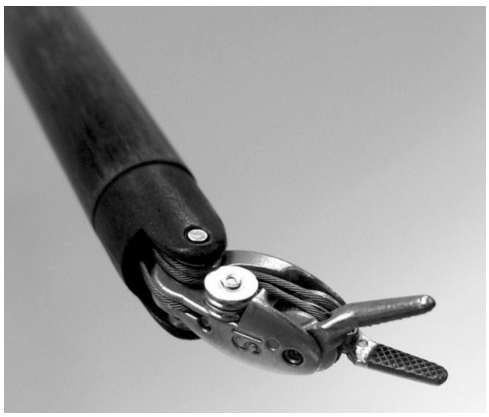

Figure 1: EndoWrist grasper used with the da Vinci robotic surgery platform. Image taken from [1].

Secondly, MIS causes severe ergonomic problems for the surgeon [4]. This is a result of the long instruments and the awkward body positioning involved in maneuvering them. Especially during longer surgeries this is problematic. This issue has lead to the development of Robot-Assisted Minimally Invasive Surgery (RAMIS) [4]. In RAMIS the surgeon is removed from the operating table and sits behind a controller from which he controls

robot arms that hold and move the instruments and endoscope. RAMIS provides more advantages than just improved ergonomics. The system is able to reject hand tremors and remove the fulcrum effect experienced in MIS. Additionally, robotic systems have been able to improve dexterity by providing extra degrees of freedom (DoF) with steerable instruments like the one shown in Figure 1 [4, 5].

There are however also some limitations associated with RAMIS. The main problem stems from the fact that, with the surgeon completely removed from the instruments, it is not possible to feel any forces exerted on the tissue. The absence of force feedback has been found to result in more frequent slips, errors and tissue damage [2]. Surgeons can also no longer use force sensation to differentiate normal tissue from a tumor through palpation. Finally, the lack of feedback has also lead to suture breakage during suturing becoming more common in RAMIS because of excessive forces being applied [4].

Many papers have already proposed the measurement or estimation of instrument-tissue interaction forces to resolve some of these problems. They include many different strategies and types of sensors to measure or estimate forces at the instrument tip.

This literature review aims to provide insight into the important considerations and limitations of force sensing in MIS as well as providing an overview and analysis of the state-of-the-art. It starts in Section 2 by discussing what different applications force sensing could be useful for. The different applications also have different requirements. What these requirements are and how they are different for each application is outlined in section 3. In the first part the requirements pertaining to sensor specifications are discussed. In the second part the dichotomy between accuracy and reusability and the influence of sensor location is discussed. In the final part other important considerations and requirements are listed.

The central part of this work is focused on reviewing the state-of-the-art of sensing in MIS. Section 4 outlines the strategy used to obtain the force sensing strategies proposed to date. The results obtained through the literature search are presented in Section 5. The included literature is divided into categories based on the type of sensing strategy they apply. The proposed solutions within each category along with their basic operating principles are presented. In Section 6 it will be evaluated whether the results agree with the requirements outlined in Section 3 and with each other. The Discussion will also discuss why it is difficult to point out a single best strategy at this time. Finally, the review concludes in Section 7 with a general overview of what has been found in this work and what it means.

2 Applications

Measuring or estimating the tip forces in MIS can be used for several different applications. The most obvious, and most commonly cited, application of these measurements is force feedback. Force feedback is most interesting in RAMIS but can also be useful in MIS. In RAMIS it can be used to physically restore the force sensation to what it would feel like in MIS. Perhaps the best solution, useful in both MIS and RAMIS, is to restore force sensation to what it would feel like without any distortion or friction losses. It is also possible to indicate the magnitude and direction of the force visually. This can be done through augmented reality by adding a force vector on the images from the endoscope.

Several studies have already found that adding physical or visual force feedback in RAMIS results in lower grasping forces, fewer errors and less tissue damage, especially for novice surgeons [6, 7, 8, 9].

The second possible application is mainly focused on the prevention of accidental tissue damage. It involves measuring or estimating the force being applied and using software to limit it to a certain value. This force limiting feature can prevent the application of excessive grip force or the accidental piercing or tearing of tissues. For example in situations when the surgeon is distracted or has a reflexive twitch-like movement or when someone accidentally bumps into the controller. Moreover, with increasingly smaller instruments being proposed, force limiting can also be used to prevent damage to the instrument. The implementation of a force limiting feature could however prove to be complicated. There are instances in which the grip force is allowed or required to be higher, for instance when grasping a needle instead of tissue. It is also possible that tissue is intentionally torn, pierced or spread during surgery. These situations will have to be somehow accounted for in the software implementation.

A final possible application is called palpation. During normal palpation a doctor or surgeon squeezes or presses into tissue in order to detect changes in stiffness or hardness. Any changes in stiffness could indicate the presence of a lump or tumor. One could for example think of feeling for lumps that may indicate breast-cancer. During surgery palpation can also be used to detect pulsating blood vessels. When the surgeon is no longer has any force feedback it is possible to press a probe into the tissue and measure or estimate the force to detect the changes in stiffness.

The different applications listed above also come with different requirements on the force sensing

strategy. What these requirements are and how they differ between the different applications will be discussed in the next section.

3 Sensor requirements

To be able to review and analyse the state-of-the-art of force sensing in MIS it is important to be aware of all the requirements, challenges, and other considerations. Due to the application in a surgical environment there are a lot of relatively strict requirements. The first part of this section focuses on the required sensor specifications. It will be explained what these sensor specifications are and how they are not the same for each different application. In the second part it is discussed how the sensor location is affected by the dichotomy between accuracy and reusability. In the final part other important considerations and requirements are listed.

3.1 Sensor specifications

There are several requirements that can be listed under the category of sensor specifications. The requirements all cover aspects related to what exactly is being measured. This includes which forces should be measured (and which not), over what force range they should be measured and with which resolution and bandwidth.

3.1.1 Required forces

The interaction forces between the instrument tip and tissue can be divided into two distinct modes; tactile and kinesthetic forces. Tactile forces are detected by receptors in the skin. They provide information about surface texture or distributed pressures. To measure these forces one requires a sensor with a high spatial resolution. Kinesthetic forces are normally detected by receptors in tendons and muscles. They provide information on the magnitude and direction of (large) external forces [10, 11]. In MIS tactile forces can be measured at the grasping surfaces. They can be used to give the surgeon a sense of how the tissue is being held, as well as the texture of the tissue. Kinesthetic forces can be used to feel how hard one is pushing, pulling or gripping the tissue or to obtain information on tissue stiffness. For the applications of force feedback, force limiting or palpation kinesthetic forces are the most interesting. Therefore, only the sensing of these forces will be considered throughout the review. Other recent reviews have focused specifically on tactile sensing and feedback [12, 13].

It is now possible to discuss the kinesthetic force components one would need to measure for the different applications. Figure 2 gives an overview of most of the forces acting on a (non-steerable) MIS instrument. A MIS grasping instrument has 5 DoF through which forces can be applied and measured: x-y translation forces caused by rotations around the incision, z forces due to translation in the longitudinal axis of the instrument, a moment around the z axis due to rotation of the instrument and finally a fifth DoF resulting from the grasping motion. Here the x-direction is parallel to the flat face of the grasper and the y-direction is perpendicular to the flat face as indicated in Figure 2. For steerable RAMIS instruments like the one shown in Figure 1 the situation is a bit more complicated. This is due to distal hinges that allow the tip to rotate around the x and y axis (also referred to as pitch and yaw). This results in a total of 7 DoF for steerable instruments.

In order to palpate tissue a probe is pressed into the tissue. By measuring the force during this interaction it is possible to determine the stiffness of the tissue and detect tumors. In the ideal case the force is always applied in the longitudinal (z) direction of the instrument requiring only a single DoF sensor. When this is not possible a 3 DoF sensor that measures forces in the x-y-z directions is needed to determine the force perpendicular to the tissue.

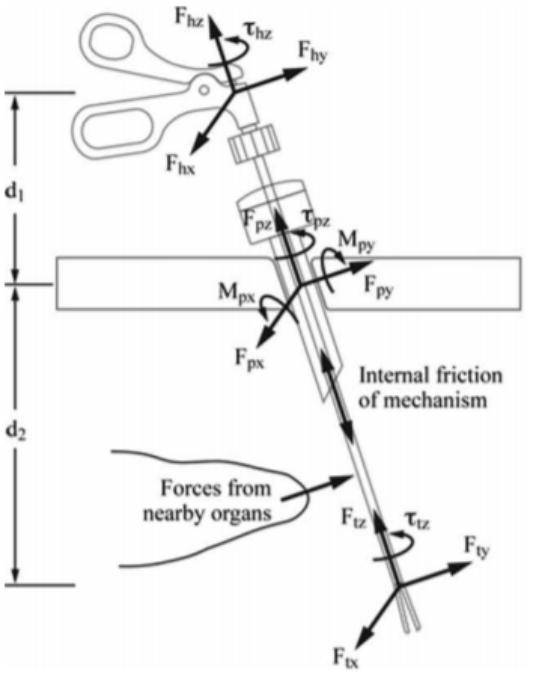

Figure 2: Schematic representation of the forces acting on a laparoscopic instrument. Figure taken from [2]

When force limiting is the objective the x-y-z forces at the tip are relevant to prevent tissue

damage from tearing or piercing. Inappropriate pinching or grip force is one of the most common errors and causes of tissue damage during MIS [14, 15]. Therefore, measuring the pinch or grip force can be a useful addition to prevent damage.

For force feedback one would quickly assume that sensors for all DoF are required. However, it has been found that partial force feedback instead of full force feedback also provides a significant improvement in surgery [16]. Some evidence even suggests that partial could be better than full force feedback [17]. The x-y-z forces along with the grip force are likely most relevant for force feedback during tissue manipulation. The moment around the Z-axis (the long axis of the instrument) can also be useful during suturing for example.

3.1.2 Force/Torque range

Due the complexity of measuring tissue interaction forces in a realistic environment it is difficult to determine the exact force range required. Two studies have found that tissue interaction forces during MIS range from 0 to about 10N and torques from 0 to 0.1Nm [18, 19]. These estimates are however based on measurements from a sensor placed near the instrument handle instead of near the tip. Why the location is relevant will be explained in Section 3.2.1.

Tissue grip forces in RAMIS have been found to range from 0 to about 4N when tissue is passed from one grasper to another [8]. A different study found that to hold tissue while a pulling force is applied grip forces may well exceed that range. The exact force however, depends on the size and texture of the grasping surface [15]. Therefore, the sensing range required for force feedback and force limiting should extend to around $\pm$10N for tip forces, at least 4N for grip forces and $\pm$0.1Nm for torques.

For palpation the force range requirement is different from the one for force feedback and force limiting. The range is dictated by the maximum force required to obtain sufficient information to distinguish tumors in tissue. It has been argued that for palpation a range of 2N suffices [11]. Not only is the maximum force required quite low, it is also generally applied with a ball-shaped probe. Therefore, there is little risk of tissue damage during palpation.

3.1.3 Force/Torque resolution

For force feedback it is possible to estimate the required force resolution by finding the smallest force change one can actually feel. One study has found that while moving the hand with an applied reference force of 1.5N the smallest noticeable difference is on average 0.68N [20]. Another study found that in a quasi-static situation the noticeable force difference from 1.5N could be as low as 0.15N depending on the direction the force is applied [21]. Considering that 1.5N is a reasonable reference in the context of MIS a minimum force resolution 0.15N is required [22].

The resolution for palpation again depends on what is necessary to resolve differences in stiffness that might indicate a tumor. The required resolution for palpation was found to be approximately 0.01N when combined with the 2N range [11].

The resolution for force limiting is somewhat arbitrary. As long as the sensor is able to detect the force limit before it is exceeded. This also depends on any safety margin programmed in the software.

3.1.4 Bandwidth

The required bandwidth or sampling frequency of the sensor can be obtained by looking into human reaction and perception bandwidth.

It has been found that 95% of grasper angle frequency content during MIS is below 2Hz [22]. However, the maximum bandwidth of human reflexive action is around 10Hz [23]. While tactile perception of vibrations can range up to $250 - 300$Hz [24, 13] we are interested in kinesthetic perception times here. Although according to Brooks [23] it is difficult to measure kinesthetic bandwidths directly, he states that estimates are in the range of $20 - 30$Hz. Since no high frequency vibrations are to be expected originating at the instrument tip, the minimum required bandwidth for this sensor application is therefore 30Hz. However, in practice it is possible that, in order to create a stable control system, higher sensor sampling frequencies are required.

The required bandwidth for palpation depends on the speed at which the probe can be moved across the tissue. For force limiting determining the required the bandwidth is a bit more complicated. It should be high enough to prevent sudden accidental force peaks that could damage the surrounding tissues. Since human reflexive actions are limited to 10Hz a bandwidth of at least this number should allow for the prevention of accidental piercing or tearing of tissue due to human twitches. However, the required bandwidth could also depend on the maximum velocity of the instrument. Imagine a situation in which the instrument is not in contact but moving very quickly due to accidentally manipulating the controller for example. When the instrument now contacts tissue the force will increase very quickly because the tissue is decelerating the instrument.

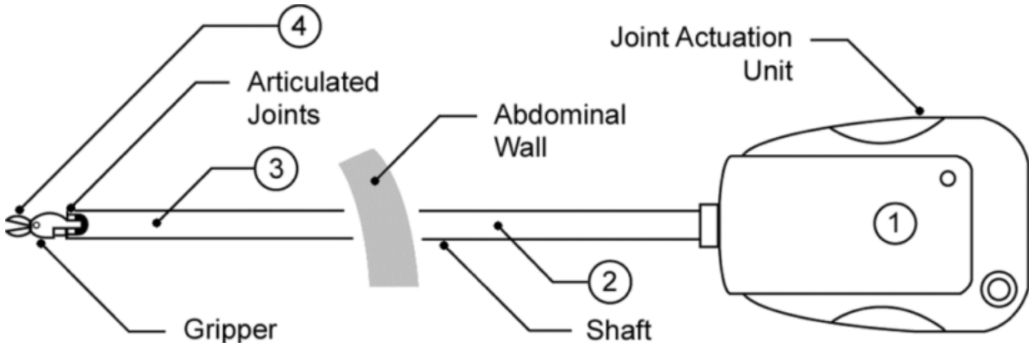

Figure 3: Overview of the possible locations to place a sensor with a instrument for RAMIS. 1: at the interface of the instrument and robot arm, 2: Proximal shaft, 3: Distal shaft and 4: Grasper tip. Figure taken from [1]

3.2 Accuracy and reusability

There are many locations from which tissue interaction forces occurring at the tip of the instrument can be measured or estimated. Figure 3 gives an overview of the possible locations to place a sensor with a instrument for RAMIS. It is possible to place a sensor at the interface between the robot arm and the instrument, or at the handle in the case of a MIS instrument (1). Next, there are several locations along the shaft were sensors could be placed; on the instrument shaft but near the handle or robotic arm (2, proximal shaft), on the shaft but inside the abdomen (3, distal shaft), in the articulated joints of the instrument (wrist), and finally at the tip or grasper of the instrument (4) [1, 2]. A final possibility is placing the sensor in the trocar and determine the tip forces trough the forces transferred from instrument to trocar. It is also possible to not place any sensor at all. Instead one could measure the forces that are generated to move or steer the instrument and estimate the corresponding tip forces.

Deciding whether, or where, to place a sensor involves a set of conflicting considerations like space, biocompatibility, sterilization and accuracy. Also the force components that one wants to measure can be of importance for the choice of location. It is for example difficult to measure the grip forces from a sensor located in the trocar. These factors, and why they are conflicting, will be outlined in the following sections.

3.2.1 Accuracy

Sensing strategies that involve no sensors at all or sensors placed near the handle or robotic effector benefit from reduced space, biocompatibility and sterility requirements. The latter two requirements will be discussed further in Sections 3.2.2 and 3.2.3. There is however also a downside to doing so. Measuring or estimating forces from outside the abdomen, particularly past the trocar, can result in significantly less accurate measurements. This is caused by forces and torques generated by friction in the trocar and instrument, the stiffness of the abdomen and the lever action of the instrument [1, 2]. These interaction forces are also illustrated in Figure 2.

The friction forces in the trocar can exceed 3N. Similarly, the torque caused by the stiffness of the abdomen when it is manipulated can range up to 0.7Nm [16, 18]. Friction in the instrument can account for losses of over 50% and significantly distort forces [16, 25]. These effects are about the same magnitude as and indistinguishable from the forces and torques we want to measure. Moreover, exact magnitude of these forces and losses can change from patient to patient and depends on the type of instrument and trocar, speed and direction of movement, temperature and whether the instrument is wet or dry [16, 25]. This combination of factors makes it exceedingly difficult to correctly model and estimate the forces at the tip.

3.2.2 Cleaning and sterilization

Surgical instruments need to be clean and sterile when they enter the OR. To achieve this instruments go through an extensive cleaning and sterilization procedure which involves hand or ultrasonic cleaning, exposure to cleaning agents (soap, detergents etc.) and finally a sterilization process at high temperature (134°C), vacuum, and 100% humidity. The fact that the instrument has to be cleaned and sterilized imposes a number of requirements on the sensor when it is mounted on the instrument. Firstly, in order be able to remove all contaminants from the sensor and instrument it should not include small open crevices. It should also be robust enough to be cleaned by hand or ultrasonically. The materials used should not react with cleaning agents, be permeable to water vapour or degrade at the sterilization temperature. Finally, since the sensor is exposed to water, blood

and cleaning agents it should be both corrosion resistant and sealed.

Not only should any sensor remain intact and functioning after a cleaning and sterilization cycle, it would also be helpful if the sensor is repeatable afterwards. In this case having a repeatable sensor means that it does not have to be re-calibrated after every sterilization cycle. Not having to re-calibrate the sensor before every use saves a lot of time in preparation before surgery.

These requirements are rather strict and difficult to meet. As a result it is not uncommon to find disposable instruments being used in laparoscopic surgery. For some instrument and devices it can also be cost effective to be disposable. However, many MIS graspers are reusable and, although they are complicated, instruments used in RAMIS are also generally semi-reusable. Since the year 2020 the reusability of the cable-driven instruments like the one shown in Figure 1 is limited to 16 times, mainly due to cleanability issues. To prevent additional cost and reduce the environmental burden it is important that sensors added to these instruments are also sterilizable.

3.2.3 Biocompatibility

If the sensor is placed on a part of the instrument that will be placed inside the body of patients the sensor will need to be biocompatible. This means that materials that come into contact with tissue or blood must not cause adverse reactions or an immune response. Therefore, materials used in the sensor or instrument that contact tissue or blood should be certified for externally communicating devices with limited duration (< 24h) contact. It is possible to choose only biocompatible materials for the sensor. However, it is also common to shield the device by applying a biocompatible coating. Since there are ample biocompatible materials and coatings for short term invasive use it is unlikely that this requirement will be a significant limitation.

3.3 Other considerations

Finally, there are some additional considerations that are important in the evaluation of sensing strategies. These include; temperature sensitivity, sensitivity to electromagnetic (EM) interference, sensor size and cost.

3.3.1 Temperature sensitivity

Most of the physical effects that can be employed to measure forces or displacements are also sensitive to changes in temperature. This means that any change in temperature will affect the force measurement in a way that is not distinguishable from the actual force measurement. Due to physiological processes, external cooling of the patient, application of flushing solutions and electronic cauterization it is likely that the temperature during surgery will fluctuate within several degrees Celsius. Therefore any proposed sensing strategy should involve a measure that mitigates temperature sensitivity.

3.3.2 EM interference

The OR is a place with a lot of different electronic devices. All of those devices can emit EM signals that can interfere with the force measurement signal and create noise. Especially when this signal has to travel from inside the patient to an interrogator placed at some distance. Moreover, bipolar instruments for electric cauterization are commonly used in surgery. These instruments are likely to form a big source of interference for any sensor placed distally. Therefore, sensing strategies that are insensitive to such EM interference should be preferred.

3.3.3 Size

Even though MIS already is a great improvement compared to conventional surgery it is still being attempted to reduce invasiveness even further. This is being done in several ways. Firstly by reducing the number of ports by performing Single Incision Laparoscopic Surgery (SILS). Secondly by using natural orifices to perform the surgery like in Natural Orifice Transluminal Endoscopic Surgery (NOTES). Finally by trying to reduce the size of the incisions in conventional MIS. All of these methods involve reducing the size of the instruments. While the EndoWrist instruments for the da Vinci platform are 8mm in diameter, other parties (like TransEnterix) are already pushing for 3mm instruments. Therefore, it is important to have a sensing strategy that is able to scale down with the size of the instrument.

3.3.4 Cost

As with most products it is important that the cost of sensorized instruments or force estimating robotic platforms is reduced as much as possible. Therefore, a sensorized instrument should be either reusable or replaceable without the entire instrument being discarded. Also the sustainability of disposable sensors or instrument is of importance in this consideration.

Not only the cost of the instrument and/or sensor are important in this consideration. Some sensing strategies might involve very expensive hardware to read-out the sensor which could increase the price of a robotic platform.

4 Search strategy

After having discussed all the important requirements and considerations for force sensing in MIS the paper will now focus on the review of the available literature. A thorough PubMed and Scopus search has been performed to obtain all the relevant literature published on force sensing strategies in (RA-)MIS. The following search term was used: *Force AND (Sensing OR Sensor) AND ("Minimally invasive surgery" OR MIS OR "Robot assisted minimally invasive surgery" OR RAMIS)*. This search query gave 146 results in PubMed and 579 in Scopus. After removing duplicates, 637 results remained. Out of those 301 relevant titles were identified.

After removing duplicates and scanning for relevant titles several inclusion and exclusion criteria were applied:

Only strategies actually integrated and tested in MIS instruments were included. Papers on sensors applied in anything other than conventional MIS (laparoscopic surgery), robotic MIS or NOTES instruments were excluded. This was done because the instruments used in these three cases have mostly similar form factors and requirements. As explained in Section 3.1.1 this review only considers kinesthetic tip force sensing. Therefore studies on tactile sensors with spatial resolution were excluded. Papers that did not include technical details and performance indicators about the force sensor, or papers that discussed earlier iterations of the same sensor were also excluded. To be able to compare the studies with each other, sensors that do not output a force measurement were also excluded. For example, a lot of palpation probes that use indentation depth or pressure (instead of force) to measure tissue stiffness were excluded. After exclusion 69 papers from Scopus and PubMed remained.

After observing keywords in the obtained literature it was concluded that some relevant search terms were missing. Therefore a second search was performed with the following search term: *Force AND (Sensing OR Sensor) AND ("Minimally invasive surgery" OR MIS OR "Robot assisted minimally invasive surgery" OR RAMIS OR Laparoscopy OR Endoscopy)*. This resulted in a number of previously undiscovered papers making the iteration a fruitful effort. 278 new results were found in PubMed and 196 in Scopus bringing the total number of papers to 1242. Combining the new results and removing duplicates yielded 428 papers and 141 relevant titles. After applying the exclusion criteria 13 papers were added to the results.

Finally, an additional 6 papers were obtained from other (review) papers, bringing the total to 88 included papers.

5 Results

The search and subsequent inclusions/exclusions resulted in 88 relevant papers that discuss force sensing strategies used in (RA)MIS. Table 1 provides a complete list of the included papers. The table includes information on the sensing method (category or type), intended use and location of the sensor. It also lists the DoF that are measured along with their range, resolution and varying measures of error as a percentage of the range. Although the papers use a wide variety of sensing strategies they can be grouped into a few different categories. The categories are based on those presented in earlier reviews and include the following [1, 2]: Resistive, Capacitive, Optical, Magnetic, Input force, Image based, Acoustic and Pressure based. The categories are mostly separated by the physical transduction method they use. Notable deviations from this division are the input force and image based categories. Especially input force strategies can involve transduction methods that would otherwise belong to a different category. However, because of the fundamentally different way these categories obtain the tip force they are placed in separate categories. Figure 4 shows how the papers listed in Table 1 are distributed over the different categories.

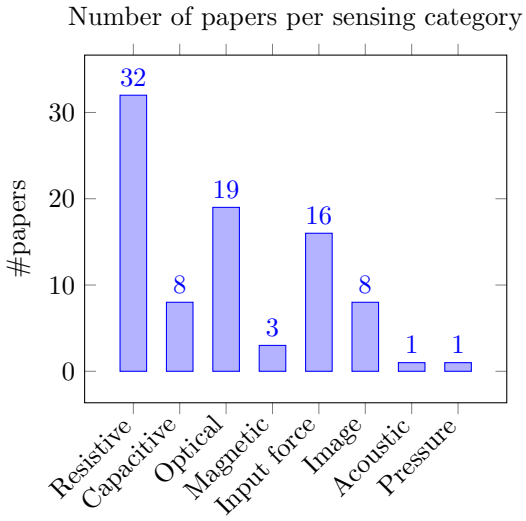

Figure 4: Distribution of included papers over the different sensor categories.

In the following sections the literature will be discussed in-depth. Each of the categories in Figure 4 will be discussed separately. The largest categories, resistive and optical, are divided further into specific sensor types. For each category and sensor type the basic principles behind their operation will be explored. The listed papers will be used to provide examples on the implementation of the respective sensor types.

Table 1: Sensing capability and performance of proposed sensing strategies applied in MIS. Locations (Loc.) are Handle (H), Proximal Shaft (PS), Distal Shaft (DS), Wrist (W), Tip (T) and In Trocar (IT). Error figures are given as a percentage of the claimed range.

Ref	**Method**	**Purpose**	**Loc.**	**DoF**	**Range [N,Nmm]**	**Resolution [mN,Nmm]**	**error [%]**
Resistive sensors							
[26]	Strain gauge	RAMIS	DS	Fx,Fy	1	100	1.2 RMS
[27]	Strain gauge	MIS	H	Fgrip	10	1	-
[28]	Strain gauge	Palpation	T	Fx,Fy,Fz	0.5(xy) 2.5(z)	-	0.3(xy) 0.6(z) RMS
[29]	Strain gauge	MIS	T	Fgrip	1.5	33	-
[30]	Strain gauge	RAMIS	PS	Fgrip	10	40	4 Max
[31]	Strain gauge	RAMIS	T	Fz,Fgrip	5	43(z) 7.4(g)	1.9(z) 0.7(g) RMS
[32]	Strain gauge	RAMIS	W	Fx,Fy,Fz, Mx,My,Mz	30, 300	-	-
[33]	Strain gauge	Palpation	DS	Fx,Fy,Fz	1.5(xy) 3(z)	15(xy) 150(z)	1.8 RMS
[34]	Strain gauge	RAMIS	W	Fx,Fy,Fz, Mx,My,Mz	10, 0.16	120(xy) 500(z), 7	-
[35]	Strain gauge	MIS	DS	Fx,Fy	13	-	4.9(x) 3.7(y) Avg.
[36]	Strain gauge	RAMIS	DS	Fx,Fy	5	55	0.5(x) 0.6(y) RMS
[37]	Strain gauge	MIS	T	Fx,Fy,Fz	5	130(x) 200(y) 50(z)	-
[38]	Strain gauge	RAMIS	PS	Fx,Fy,Fz, Mx,My,Mz	9	-	-
[39]	Strain gauge	NOTES	T	Fgrip	16	-	1.1 RMS
[40]	Strain gauge	MIS	DS	Fx,Fy,Fz	10	-	7.5(x) 9(y) 50(z) RMS
[41]	Strain gauge	MIS	DS	Fx,Fy	5	200	1.8 RMS
[42]	Strain gauge	RAMIS	W	Fx,Fy,Fz, Mx,My,Mz	10, 10	-	-
[43]	Strain gauge	MIS	T	Fx,Fy,Fz, Fgrip	2.5	10	0.9(xy) 0.1(z) 3.7(g) RMS
[44]	Strain gauge	NOTES	PS	Fz, Mz	40, 0.7	300, 10	0.8, 2.5 RMS
[45]	Piezoresistor	MIS	PS	Fx,Fy,Fz Mx,My,Mz	35(xy) 106(z), 1.5(xyz)	-	0.9, 0.5 Max
[46]	Piezoresistor	MIS	DS	Fx,Fy,Fz	2.6	5	4
[47]	Piezoresistor	MIS	T	Fgrip	10(g)	500	12.6 Avg

Ref	Method	Purpose	Loc.	DoF	Range [N,Nmm]	Resolution [mN,Nmm]	error [%]
[48]	Piezoresistor	RAMIS	T	Fx,Fy,Fz	0.05(xy) 0.03(z)	0.02(xy) 0.05(z)	-
[49]	Piezoresistor	Palpation	T	Fz	1	-	0.4 RMS
[50]	Piezoresistor	MIS	T	Fx,Fy,Fz	1.5(xz) 5(y)	10(xz) 17(y)	-
[51]	Piezoresistor	MIS	T	Fgrip	20(g)	-	-
[52]	Piezoresistor	RAMIS	PS	Fx,Fy,Fz	9(xy) 20(z)	60	0.7(xy) 0.3(z) Max
[53]	Piezoresistor	MIS	T	Fx,Fy,Fz	25	125	-
[54]	Piezoresistor	MIS	T	Fx,Fy,Fz	3(xy) 50(z)	40(xy) 50z)	-
[55]	Piezoresistor	Palpation	T	Fx,Fy,Fz	0.001	0.003	-
[56]	Piezoresistor	RAMIS	IT	Fx,Fy,Fz, Mx,My,Mz	36, 0.5	2, 0.025	0.6 , 1.6 Max
[57]	FSR	Palpation	T	Fx,Fy,Fz	8	100	-
Capacitive sensors							
[58]	Capacitive	RAMIS	T	Fx,Fy,Fz	8(xy) 4(z)	250(x) 1450(y) 55(z)	-
[59]	Capacitive	MIS	T	Fx,Fy,Fz, Fgrip	2.5(xz) 5(yg)	72(x) 58(y) 42(z) 46(g)	4.4(x) 1.4(y) 3.2(z) 2(g) RMS
[60]	Capacitive	Palpation	T	Fx,Fy,Fz, Mx,My,Mz	1.5(xyz), 20(xy) 10(z)	0.2(x) 0.3(y) 0.1(z), 0.5e-3(x) 0.4e-3(y) 0.2e-3(z)	3.1(x) 4.5(y) 8.9(z), 2.2(x) 2.5(y) 3.4(z) Avg.
[61]	Capacitive	RAMIS	T	Fx,Fy,Fz, Fgrip,Mz	5,0.5	2(xyg) 4(z)	3.4(x) 6.4(y) 8.6(z), 5.7 Avg.
[62]	Capacitive	RAMIS	W	Fx,Fy,Fz	1(xy) 1.6(z)	100(xyz)	.8(x) .7(y) .4(z) RMS
[63]	Capacitive	Palpation	T	Fx,Fy,Fz	5	-	-
[64]	Capacitive	Palpation	T	Fx,Fy,Fz	1	-	1.9
[65]	Capacitive	Palpation	T	Fz	0.6	0.2	-
Optical sensors							
[66]	Optical (LIM)	MIS	T	Fgrip	2	2	6 MAE
[67]	Optical (LIM)	RAMIS	DS	Fx,Fy,Fz	6	-	-
[68]	Optical (LIM)	RAMIS	IT	Fx,Fy	20	-	12 Max
[69]	Optical (LIM)	RAMIS	PS	Fx,Fy	10	200	1.5 Max

Ref	Method	Purpose	Loc.	DoF	Range [N,Nmm]	Resolution [mN,Nmm]	error [%]
[70]	Optical (LIM)	MIS	T	Fz	10	200	-
[71]	Optical (LIM)	Palpation	T	Fz	7	-	-
[72]	Optical (LIM)	RAMIS	DS	Fx,Fy	4	-	3(x) 2.8(y) RMS
[73]	Optical (LIM)	RAMIS	DS	Fx,Fy,Fz	1.7(xy) 2.5(z)	40	-
[74]	Optical (LIM)	Palpation	DS	Fx,Fy,Fz	1.5(xy) 3(z)	20	1 RMS
[75]	Optical (FBG)	RAMIS	W	Fx,Fy,Fz	12	60	0.5 Max
[76]	Optical (FBG)	RAMIS	DS	Fx,Fy,Fz, Mx,My,Mz	20, 0.15	-	5.1 Mean
[77]	Optical (FBG)	NOTES	DS	Fz	20	-	2 RMS
[78]	Optical (FBG)	Palpation	T	Fx,Fy,Fz	2	200	1.3(x) 0.3(y) 0.5(z) Avg.
[79]	Optical (FBG)	Palpation	T	Fz	5	2.6	-
[80]	Optical (FBG)	RAMIS	DS	Fx,Fy	10	50	-
[81]	Optical (FBG)	Palpation	T	Fz	7	9.3	1.7 RMS
[82]	Optical (FBG)	RAMIS	W	Fx,Fy,Fz	10	50	1 Max
[83]	Optical (FBG)	MIS	DS	Fx,Fy,Fz, Fgrip	5(xyz) 20(g)	50	4(xyz) 3.8(g) RMS
[84]	Optical (FBG)	MIS	T	Fz,Fgrip	6(z) 10(g)	40	5(z) 2.7(g) RMS
Magnetic sensors							
[85]	Magnetic (LVDT)	Palpation	PS	Fz	3	-	4.4 Max
[86]	Magnetic (Hall)	MIS	T	Fy,Fz	7(y) 35(z)	6	-
[87]	Magnetic (Hall)	Palpation	T	Fz	1	4	-
Input force sensors							
[88]	Input force	RAMIS	NA	Fgrip	1.8	-	3.3 MAE
[89]	Input force	RAMIS	NA	Fx,Fy	9	-	8.3 MAE
[90]	Input force	RAMIS	NA	Fx,Fy,Fz	5	-	7.4 Max
[91]	Input force	RAMIS	NA	Fx,Fy,Fz	5	-	16(x) 12(y) 4(z)

Ref	Method	Purpose	Loc.	DoF	Range [N,Nmm]	Resolution [mN,Nmm]	error [%]
[92]	Input force	NOTES	NA	Fx,Fy,Fz	3.5	-	0.6 RMS
[93]	Input force	RAMIS	NA	Fgrip	1	-	23 Max
[94]	Input force	NOTES	NA	Fx,Fy,Fz	4	-	6.3(xz) 3.8(y) Max
[95]	Input force	Palpation	NA	Fx,Fz	3	-	14.7
[96]	Input force	RAMIS	NA	Fx,Fy,Fz, Fgrip	1(xyz) 0.6(g)	-	10(xyz) 13(g) MAE
[97]	Input force	RAMIS	NA	Fx,Fy,Fz	-	-	2.3(x) 3.2(y) 3.3(z) RMS
[98]	Input force	RAMIS	NA	Fgrip	2.5	-	6 Max
[99]	Input force	RAMIS	NA	Fgrip	3	-	17 Max
[100]	Input force	RAMIS	NA	Fgrip	12	-	3.3 Avg
[101]	Input force	RAMIS	NA	Fx,Fy,Fz, Mx,My,Mz	-	-	5.4(x) 3.4(y) 0.1(z), 0.1(x) 0.5(y) 0.1(z) RMS
[102]	Input force	RAMIS	NA	Fx,Fy, Fgrip	4	150(xy) 100(g)	7.3(x) 6.1(y) 10.6(g) Avg
[103]	Input force	RAMIS	NA	Fx,Fy, Fgrip	2	-	22 Max
Image based sensors							
[104]	Image based	RAMIS	NA	Fx,Fy,Fz	10	-	0.2 RMS
[105]	Image based	Palpation	NA	Fx,Fz, Fgrip	1	-	5.4
[106]	Image based	RAMIS	NA	Fz	200	-	0.43 Avg
[107]	Image based	RAMIS	NA	Fz	2.5	-	60
[108]	Image based	NOTES	NA	Fgrip	1	-	-
[109]	Image based	RAMIS	NA	Fx,Fy,Fz, Mx,My,Mz	10, 5	-	0.6(x) 0.4(y) 9(z), 2.4(x) 2.6(y) 0.2(z) RMS
[110]	Image based	RAMIS	NA	Fx,Fy,Fz	2.5	-	2.8 RMS
[111]	Image based	Palpation	NA	Fz	0.3	10	-
Acoustic sensors							
[112]	Acoustic	palpation	T	Fx, Fz	0.75(x) 5(z)	20(x) 23(z)	7.2(x) 4.2(z) RMS
Pressure based sensors							
[113]	Pressure based	Palpation	DS	Fy	5	-	4.8 RMS

5.1 Resistive sensing

As Figure 4 shows, the resistive sensing category is by far the most common in literature. This is mainly due to the size and simplicity of included sensors which consequently makes them relatively cheap. The resistive sensing category can be divided into metallic strain gauges, piezoresistors and Force sensing resistors (FSRs). These sensor types are distinguished by the effects that generate their output. The following sections will explain this further and discuss the included literature.

5.1.1 Metallic strain gauge

As listed in table 1 there are 19 examples in literature of strain gauges used to measure forces in (RA)MIS. Metallic strain gauges generally use a metallic wire film attached to the surface of an object. They detect a change in resistance when the object is subjected to strain. To minimize the sensitivity to lateral strain most strain gauges come in a zig-zag pattern as is shown in Figure 5 [114]. All but one of the strain gauge sensors in Table 1 come in this shape.

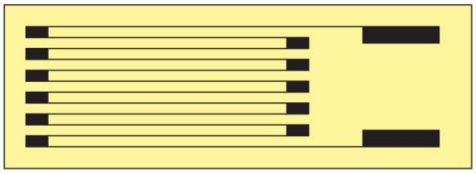

Figure 5: Example of a thin film strain gauge with bond pads to the right and the zig-zag sensing region to the left. Figure taken from [115].

To understand what causes the change in resistance when strain is applied we look at the equation for resistance (R) through a conductor:

$$R = \frac{\rho L}{A} \tag{1}$$

where ρ is the resistivity of the material, l is the length of the conductor and A is the cross sectional area of the conductor. Taking into account the Poisson ratio (ν) a relative change in resistance can be expressed as follows [115]:

$$\frac{dR}{R} = \frac{dL}{L}(1 + 2\nu) + \frac{d\rho}{\rho} \tag{2}$$

Equation 2 shows that the change in resistance can be caused by a change in length, multiplied by the change in cross-sectional area due to the Poisson effect, or a change in resistivity. The sensitivity of a strain gauge to a relative change in length (strain), commonly called the gauge factor (GF) is expressed by [114, 115]:

$$GF = \frac{dR/R}{dL/L} = (1 + 2\nu) + \frac{d\rho/\rho}{dL/L} \tag{3}$$

For most metals the gauge factor ranges from 2 to 3 and is almost exclusively the result of the change in length and cross-section. This is also called the geometric effect [115, 114].

The simplest way to implement strain gauge sensors is to place them on the instrument handle [27]. It is also possible and simple to place them on the outer shaft of the instrument and measure strain from tip forces transferred to the shaft [36, 39, 40]. In a similar approach three other examples have placed the strain gauges on a separate part they call a sleeve which is placed around the instrument [26, 35, 41]. The advantage of implementing the strain gauges in such a way is that they are separate from the instrument. Therefore even when the gauges cannot be sterilized most of the instrument can still be reused. The downside of such a system is that accuracy of the measured forces depends on the tolerance of the fit between the sleeve and the instrument. Any gap will result in a dead-zone in which no force is recorded.

Most of the other papers have used a different approach. To ensure that the strain gauges are strained in only one direction they have been integrated into compliant structures. Some of the compliant structures are integrated in the shaft of the instrument [32, 33, 44], others in the wrist section [34, 42] and still others are placed at the tip [29, 28, 31, 37, 43]. Figure 6 shows an example of a compliant structure located at the tip as proposed by Yu et al. [43]

Strain gauges are not only sensitive to strain, they are also sensitive to temperature. In metallic strain gauges the main cause of this sensitivity is thermal expansion. Thermal expansion influences the resistance when the strain gauge and the object it is bonded to do not expand equally. This can occur when they are made from different materials with different thermal expansion coefficients or when there is a temperature gradient [114, 115]. As mentioned in Section 3.3.1 the temperature during surgery is not constant and can therefore result in errors. A well known solution for temperature compensation are Wheatstone bridges, also commonly referred to as bridge circuits. Temperature compensation is not the only reason Wheatstone bridges are useful though. The bridge circuit is also able to improve the sensitivity and SNR [115].

To help explain how the bridge works Figure 7 shows a schematic representation of a full Wheatstone bridge. When all the resistances ($Z_1 ... Z_4$) are equal the output voltage V_0 equals zero. When one of the resistances changes the voltages V_1 and

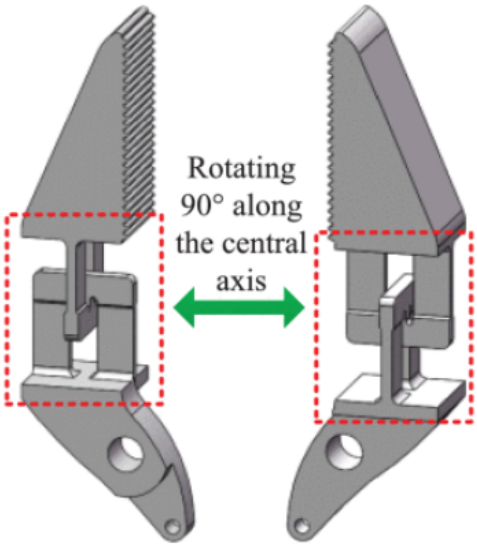

Figure 6: Example of a compliant structure for the application of strain gauge sensors. Figure adapted from [43].

V_2 are no longer equal and V_0 will become non-zero [116]. Because of the small GF in metallic strain gauges mentioned earlier the change of resistance is only a few percent. Therefore measuring this change as a deviation from zero through a bridge circuit provides improved sensitivity and SNR.

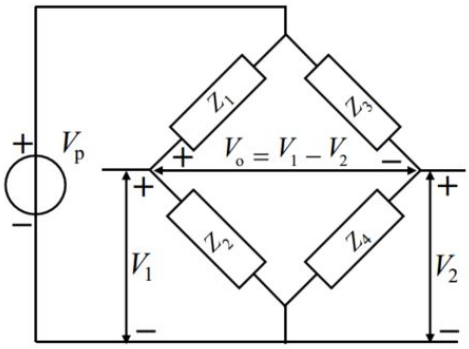

Figure 7: A Wheatstone bridge circuit consisting of four resistors and a voltage source. When the resistance of one of the resistors changes the differential voltage output V_0 changes. Figure taken from [116].

Temperature compensation using a bridge circuit is based on the principle that the output voltage remains unaffected as long as $Z1/Z2 = Z3/Z4$. So when Z_1 and Z_2 are identical strain gauges that are at the same temperature the ratio $Z1/Z2$ will remain unchanged and the temperature sensitivity is greatly reduced. To actually have the same temperature both strain gauges are generally placed near each other on the test specimen [116, 115]. These so called half-bridge configurations are very common in resistance based sensing.

It is possible to further improve the sensitivity by placing the two strain gauges such that they are strained in opposite directions. This can for example be done by placing one on the top and the other on the bottom of a beam loaded in bending. One strain gauge is now loaded in tension and the other in compression. The result is a sensitivity that is approximately twice as high compared to only one strain gauge being loaded [116, 115]. Almost all of the listed papers using strain gauges have applied full- or half-bridge circuits to compensate for temperature or improve sensitivity.

Table 1 shows that there is a big spread in sensing range among the strain gauge sensors. The highest is 40N [44] and the lowest is 1N [26]. Based on our requirements the former is higher than required for most RAMIS procedures and the latter is too low. Nonetheless, ranges around 10N are also listed frequently [27, 30, 93, 35, 38, 40, 42].

The resolution figures show a similarly large spread. Moreover, Table 1 shows that a smaller range allows for a smaller resolution and vice versa. Unsurprisingly, the highest resolutions are found among the papers that have implemented the strain gauges with a Wheatstone bridge.

In terms of relative error the same effect can be observed; A larger range results in a larger relative error. One of the included papers by Trejos et al. listed in Table 1 shows a very high error. However, it must be added that those error figures were obtained after several sterilization cycles [40]. While most others do not mention sterilization or state to have designed a disposable sensor only a few claim that their sensor is (potentially) sterilizable [26, 27, 30, 35, 40, 43]. Only Trejos et al. and Fahkry et al. have actually investigated the performance of strain gauges after autoclave sterilization. Trejos et al. constructed several types of strain gauges with different adhesives and coatings to find the best combination for sterilization. Their prototype was able to survive 6 sterilization cycles. Nonetheless, it can be questioned whether the error is acceptable and the sensor needs to be calibrated after every cycle as well [40]. Fakhry et al. were able to sterilize there sensor, located at the instrument handle, 10 times with calibration performed after the first, fifth and tenth sterilization and without deterioration [27]. Their sensor is also the only one tested during *in vivo* human surgery.

5.1.2 Piezoresistors

Out of the 32 sensors in the resistive category 13 involve Piezoresistive strain gauges. Piezoresistive strain gauges, also known as semiconductor strain gauge, microstrain gauge or piezoresistor, work in

much the same way as metallic strain gauges. However, piezoresistors are made from semiconductor materials, mostly silicon, and are able to reach gauge factors of over 100. This makes them useful in situation with high noise levels or little strain. From the resolution figures listed in Table 1 it is clear that Piezoresistive sensors are indeed more sensitive compared to conventional strain gauges.

The high gauge factor is the result of the piezoresistive effect. This effect is caused by the redistribution of charge carriers between different lattice structure directions and energy bands when the lattice is deformed by strain. The redistribution leads to an increase or decrease of the resistivity ρ depending on the main energy carrier in the silicon material. The energy band structure is different in different lattice structure directions. Therefore, the size of the effect also depends on the direction in which strain is applied. Finally, the piezoresistive effect is also non-linear with strain [117]. However, for small forces and strain levels a linear approximation can be applied for calibration. Which is why only one of the listed papers describes a non-linear calibration curve [46].

The gauge factor is highest in silicon with low doping levels [115, 117]. This can be explained by the fact that when there is a small number of charge carriers the redistribution of only a few is a relatively large change. When there are a large number of carriers the relative effect due to redistribution is much smaller [117]. On the downside, the low doping level also results in a much higher temperature sensitivity for piezoresistors compared to strain gauges. This a result of the fact that temperature also affects the distribution of charge carriers between energy states [114, 117].

Similar to metallic strain gauges the temperature sensitivity can be effectively compensated through the use of bridge circuits. Most of the sensors listed have implemented full or half bridge circuits [45, 46, 49, 50, 51, 52, 53, 55, 56].

The fact that piezoresistors are made from semiconductors like silicon also provides advantages other than the high sensitivity. Using silicon as the transducer material allows for the use of micromachining processes commonly used for MEMS devices. Consequently it is possible to make these piezoresistive sensor structures very small and relatively cheap. Several of the proposed sensors listed in Table 1 have been produced using these micromachining processes [48, 50, 51, 54, 55].

Not all papers have proposed custom designed and produced sensors. Four of the papers listed in Table 1 have implemented off-the-shelf piezoresistive force sensors. Anderson et al, Latt et al. and Schwalb et al. [45, 49, 52] have placed off-the-shelf sensors at the proximal part of the instrument near the actuators. Zemiti et al.[56] have proposed an off-the-shelf sensor to be integrated in a trocar. By doing so the relatively expensive sensors are subject to less stringent sterility requirements and could therefore be reusable. These are not the only sensors that are (potentially) reusable. A few have used biocompatible coatings to make their sensors both biocompatible and sterilizable [46, 50, 51]. Other papers included in Table 1 have not mentioned the sterilization requirement.

5.1.3 FSR sensor

Only one FSR sensor has been included in Table 1. However, since it works in a fundamentally different way from both metallic strain gauges and piezoresistors it is discussed separately.

The FSR sensor used by [57] consists of three layers. The first layer contains fully conductive sensing electrodes. The second layer consists of a semiconductive composite polymer that contains conductive particles. The third layer is a common reference electrode. So current has to flow through the semiconductive polymer to obtain a signal.

The sensor works as follows. When no load is applied the conductivity of the polymer is low and the resistance is high. With the application of a load the polymer layer is compressed and its conductive particles are closer together. As a result there is an easier path for the electrons to travel through the polymer which increases conductivity and reduces the resistance. Through calibration the reduction in resistance can be related to the force being applied. By using four sensing electrodes Li et al. are able to measure forces in 3 DoF [57]. Contrary to strain gauges which only change their resistance a few percent FSRs can change their resistance a few orders of magnitude. The high sensitivity voids the need for any bridge circuit that is necessary for strain gauges [118].

Other than being highly sensitive FSRs are also very robust and able to work at temperatures of up 170^{circ}C while being relatively insensitive to humidity [57, 118]. Although not explicitly stated this means that these sensors are likely sterilizable.

Li et al. provide no accuracy figure to compare their sensor to other resistive sensors. However, in experimental testing on a tissue phantom their sensor, used as a probe, was able to produce a stiffness map very similar to one produced by an off-the-shelf reference sensor [57].

5.2 Capacitive sensing

A capacitive force or displacement sensor measures a change of the capacitance between two flat plate electrodes separated by a gap. The capacitance (C) between the two electrodes can be given by:

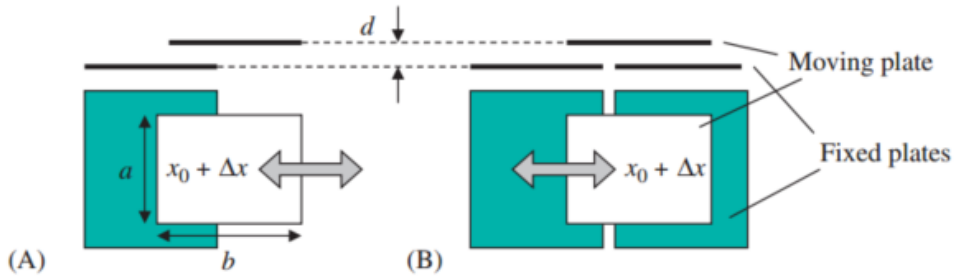

Figure 8: Variable-area type capacitive displacement sensors in (A) normal and (B) differential configuration. Figure taken from [115].

$$C = \frac{A\epsilon}{d} \tag{4}$$

With A the overlapping area of the two plates, d the distance between the plates and ϵ the permittivity. Important to note is that the permittivity depends on the material between the electrodes as well as the temperature and frequency [115].

From equation 4 it is clear that the capacitance is affected when the area, distance or permittivity between the plates changes. Since the distance d is generally very small and the relation is inversely proportional the capacitance is much more sensitive to a change in the distance. However, the fact that the distance is inversely proportional to the capacitance also means that the output is non-linear, especially for large displacements.

The high sensitivity of variable distance measuring is the reason why all but one of the capacitance sensors in Table 1 use it to measure forces [59, 60, 61, 62, 63, 64, 65]. In order to cope with the inherent non-linearity some use a calibration procedure that fits an exponential function to the sensor output [60, 61]. Others fit a linear approximation or which should suffice for smaller displacements [58, 59, 62].

Dai et al. take a different approach. Instead of choosing for either variable distance or variable area sensing they use a hybrid system. Variable distance electrodes are used to measure normal forces and variable area electrodes are used to measure shear forces [58].

To improve the sensitivity of the variable area electrodes Dai et al. have used a differential setup [58]. Figure 8 shows the difference between a normal (A) and a differential configuration (B) for a variable area sensor. In the differential setup there are three parallel electrodes. There are two distinct capacitances. One between the top and left electrode and one between the top and right electrode. These capacitances are subtracted such that when the top electrode is in the middle above the other two the output is zero. When the top electrode moves to the right the capacitance with the right electrode increases but decreases with the left electrode. Now the output is no longer zero and has changed twice as much compared to a non-differential setup. The result is a linearized change in capacitance for small displacements. Because the system now measures changes as a deviation from zero, as well as the output doubling, a differential setup is much more sensitive. The differential setup is also able to compensate for sources of interference that act on both capacitances. For example a parasitic change of distance, temperature or frequency [115, 119]. It is still important to reduce the amount of parasitic movements for example through a compliant structure that only allows displacement in the required direction.

Nagamoto et al. and Nakadegawa et al. have both constructed a completely different type of capacitive sensor [63, 64]. Instead of flat plate electrodes they use cylindrical electrodes. The electrodes consist of liquid metal contained microfluidic channels etched in PDMS. They both work in a variable distance mode, but due to the cylindrical electrodes the output is linear [63, 64].

A final important consideration for capacitive sensors is the high sensitivity to electromagnetic interference. Because most capacitors have very small capacitances (in the order of pF-nF) their output current is also very small, even at high excitation frequencies [116, 115]. This makes capacitive sensors very sensitive to other electric fields like those caused by electronic devices or even between the wires leading to and from the sensor. The influence of this source of error can be mitigated through shielding and by placing the processing electronics near the sensor [116]. Almost all of the examples in Table 1 have protected their sensor from EM interference by doing exactly that. They have shielded the sensing electrodes and placed the capacitive to digital converter (CDC) close to them. This means that the CDC had to be placed at or near the tip of the instrument. As a result none of these sensors is reusable.

Table 1 shows that while some of the included capacitive sensors have a very high resolution the force range is generally limited. The accuracy shows

a great variation with some less than 95% [60, 61] and another more than 99% accurate [62].

5.3 Optical sensing

Optical sensing strategies are distinguished by the use of light to measure displacements and forces. Many different types of optical sensors exist but not all of them are useful in the context of (RA)MIS. The two types that have been proposed extensively for use in surgical instruments are light intensity modulating (LIM) and Fiber Bragg Grating (FBG) sensors. The basic physical functioning behind these two types and the associated literature will be discussed in the following sections.

5.3.1 Light Intensity Modulating sensor

LIM sensors measure changes in light intensity from a displacement or a force. LIM sensors are the most simple and cheap type of optical sensor. Their simplicity stems from the fact that they measure intensity irrespective of frequency or phase. Consequently, they can use low coherence light sources and simple light detectors [120]. However, they are not as sensitive as interferometric or FBG sensors [115, 120, 121]. Table 1 includes 9 papers that have proposed LIM sensors in (RA)MIS. They include several different methods to influence the intensity of light.

With 7 out of 9 examples using this method, changing the distance the light travels from emitter to detector is by far the most popular method [67, 68, 70, 71, 72, 73, 74]. The distance can be altered by moving the detector with respect to the emitter or, more commonly, by moving a mirror that reflects the light away from both as illustrated in Figure 9 [122, 115, 121].

These sensors work because the inverse square law dictates that the intensity of light is inversely proportional to the square of the distance. This happens because with a diverging light beam fewer photons hit the detector when it is placed at a larger distance. When the light is reflected back to the detector by a mirror the intensity can even become inverse to the fourth power of the distance [115].

The simplest example of this kind of LIM sensor uses only one light beam and measures forces in a single DoF. Generally the light sources and detectors are placed far from the transducer (the moving mirror). The light is transmitted to and from the transducer by optical fibers. This can be done as shown in Figure 9 using separate transmitting and receiving fibers [71]. Alternatively a single fiber with an optical coupler can be used [70]. To measure forces in 3 DoF the displacement of the mirror needs to be measured on three locations. As in Figure 9 this is done by placing the fiber (pairs) 120 degrees apart [67, 73, 74].

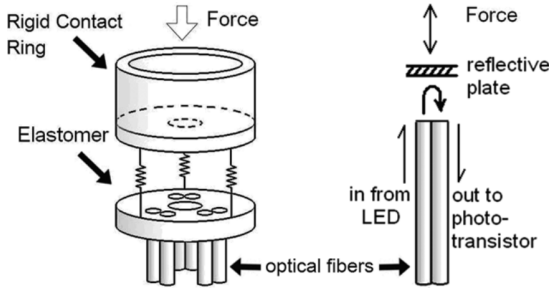

Figure 9: Example of a variable distance intensity modulating sensor. Figure taken from [123].

It is also possible to use no optical fibers at all. In this case the light source and detector are mounted radially. The light is reflected by reflectors mounted at a smaller radius around the long axis. For example Fontanelli et al. proposed a system with optical sensors mounted radially in a trocar. The light is reflected by a bronze ring around the instrument [68]. Noh et al. have used a similar configuration to measure the radial forces acting on a flexible manipulator for RAMIS [72].

A different way to modulate the light intensity for force measuring was proposed by Hosseinabadi et al. [69]. In their sensor an optical slit is placed on the proximal part of the instrument shaft between the light source and detector. When the instrument is deflected due to a force the slit moves with respect to the light beam. In doing so it will block some of the light from passing through. This change is measured by the light detector.

The final light modulation method alters the intensity by bending the fiber that conducts the light. Bandari et al. [66] have used this method to construct a sensor that measures grip forces in a MIS grasper. Their design uses an optical fiber placed below a deformable grasping surface. When a grip force is applied the deformation pushes into the fiber causing it to bend and reduce the intensity [66]. To explain how bending of the fiber reduces the intensity we have to look at the construction of an optical fiber and how it conducts light. The cladding material that surrounds the core as shown in Figure 10 generally has a lower index of refraction compared to the core. This results in an interface at which either internal reflection or refraction can occur. In a straight fiber light travels mostly at large angles of incidence to the interface (θ_3 in Figure 10). Therefore it is able to reflect from side to side through the fiber without losing intensity [122].

When the fiber is bent as shown in Figure 11, the angle of incidence is reduced. At a certain angle, called the angle of total internal reflection, the light is no longer fully reflected. When the an-

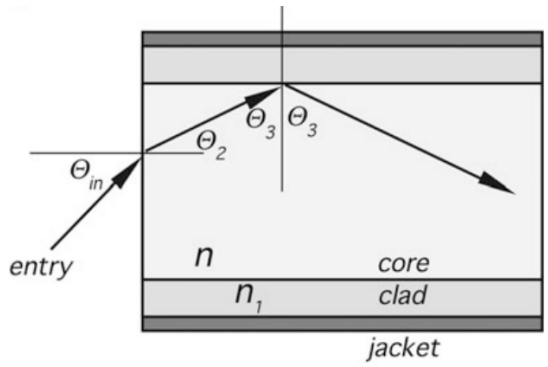

Figure 10: Illustration of the construction of an optical fiber as well as the reflection of light in an optical fiber. Figure adapted from [122].

gle of incidence becomes smaller than the angle of total internal reflection light is refracted into the cladding material, following direction y instead of x in Figure 11, and its energy is lost. Therefore, bending the fiber, especially over small radii, leads to more losses in the fiber and a reduced intensity measured at the detector [122, 120].

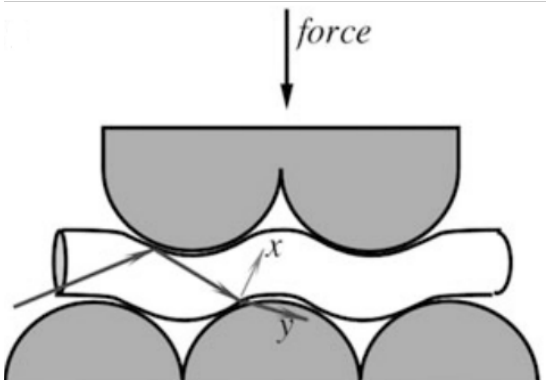

Figure 11: Illustration of a fiber bend intensity modulating sensor. When the angle of incidence becomes too small light is refracted along y instead of reflected along x. Figure adapted from [122].

The methods discussed provide relatively simple modulation of the light intensity. However, almost all of these mechanisms are affected by parasitic changes of the intensity. For example when an applied axial force also causes a change in tilt of the mirror or when fluctuations in the light source occur. Similarly, the optical fiber bending somewhere along its length can cause unwanted changes in intensity. All of these effects are indistinguishable from the actual measurand [115, 120, 121]. Most of these inaccuracies can compensated by adding a reference fiber that is subjected to the same parasitic effects but not the measurand [121]. This works in a similar way as temperature compensation with an additional strain gauge in a bridge circuit. A reference fiber was included in some of the designs that used optical fibers [67, 70, 73, 74].

Also similar to the strain gauge sensors, the LIM sensors in Table 1 show a large spread in force range. For this kind of sensors the force range is mainly determined by the stiffness and the range of motion of the measured displacement. This also results in the fact that an increased force range results in a lower resolution since a similar force now produces a smaller displacement.

5.3.2 Fiber Bragg Grating

Because FBG sensors are biocompatible, likely sterilizable and EM insensitive they have been proposed for many different biomedical applications [124, 120, 125]. Table 1 includes 10 papers that use FBG sensors in (RA)MIS. For all of them the operating principle of the FBG is the same.

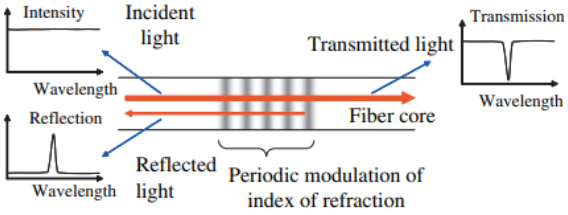

Figure 12: Operation of a Fiber Bragg grating sensor. Figure taken from [126].

As shown in Figure 12 FBG sensors are completely contained within an optical fiber which makes them very small and robust. The sensing region of a FBG is created by periodically modulating the index of refraction resulting in a grating. As a result FBGs act like the optical equivalent of a bandpass filter reflecting only a small peak of light (see Figure 12. The wavelength of the light that is reflected back λ_B is called the Bragg wavelength and is given by [120, 125, 127]:

$$\lambda_B = 2n_{eff}\Lambda \tag{5}$$

Here, n_{eff} is the average effective index of reflection in the sensing region and Λ is the grating pitch.

FBG sensors work by detecting a shift of the Bragg wavelength caused by a change of grating pitch due to applied strain. Because they measure wavelength shift instead of intensity they are not susceptible to intensity inference caused by fiber bending or light source variability. However, measuring the light spectrum instead of the intensity is more complex and costly.

FBG sensors are not only sensitive to strain, they are also very sensitive to changes in temperature. The temperature sensitivity is caused by thermal expansion changing the grating pitch

and the thermo-optic effect changing the index of refraction. These effects are large enough that FBGs can also be used as temperature sensors [124, 127]. Since the temperature is not constant during surgery this can become a large source of error. To compensate for the thermal sensitivity some have added a reference fiber to their design [76, 77, 82, 83]. The reference fiber uses a FBG sensor that is placed close the the sensing regions of the other fibers but not subjected to strain.

A single FBG sensor can only measure strain in its longitudinal direction. Therefore, measuring forces in multiple directions requires several FBGs. To do so most of the examples include compliant structures. These structures allow displacements in the required directions while constraining movement in all others. The structures help arrange the FBGs in a way to measure the required forces without any crosstalk or parasitic effects [75, 79, 81, 82, 84]. Some others have fixed the FBGs directly on or in the instrument without the use of compliant structures [78, 80, 83]. When one wants to measure forces in 6 DoF it is no longer necessary to have any additional constraints. Therefore, Haslinger et al. have proposed a sensor that uses 6 FBGs as the legs of a Stewart platform [76]. Lai et al. have used FBGs to measure forces acting in a tendon-sheath mechanism used to steer a NOTES instrument [77].

Both Lai and Haslinger make use of one of the unique advantages of FBGs namely the possibility of multiplexing [76, 77]. Multiplexing allows for the placement of multiple FBGs in the same fiber, or similarly the transmission of multiple FBG signals through the same fiber. This is possible when the FBGs have a different Bragg wavelength such that their output spectra do not overlap [122, 116, 121, 120].

Looking at the performance figures in Table 1 it is clear that FBG sensors in general are able to achieve high resolutions over large force ranges. Moreover, almost all of them are more than 95% accurate and five of them are more than 98% accurate.

5.4 Magnetic sensing

Magnetic sensors use magnetic fields created by permanent magnets or through induction to measure displacements and forces. Popular types of magnetic sensors include Hall sensors, magnetoresistive (MR) sensors and inductive (LVDT) sensors. The operation of these types of sensors and the included literature will be discussed separately in the next two sections.

5.4.1 Hall/magnetoresistive sensor

Hall sensors and MR sensors are both technically magnetic field sensors. However, the magnetic field density B decreases with increasing distance from the source. Therefore they can also be used to measure displacements and forces.

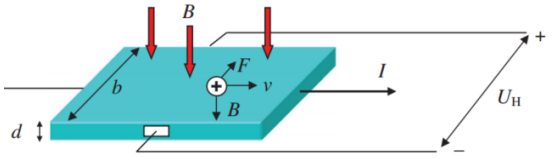

Figure 13: Illustration of a hall plate sensor. Figure taken from [115].

Hall sensors and magnetoresistors both work through the same phenomenon [122, 128]. Both sensors generally come in the shape of a plate with thickness d that has a current (I) passing through it. When a magnetic field (B) is applied perpendicular to this plate an electromotive force (F), commonly known as the Lorentz force, will cause passing electrons to move in the transverse direction. This is illustrated in Figure 13. The deflected electrons cause a transverse potential called the Hall voltage (U_H) which can be calculated using the following equation [115, 128]:

$$U_H = \frac{R_H I B}{d} \tag{6}$$

The Hall coefficient R_H equals $1/nq$ where n is the carrier density of the material. In most materials the majority of the carriers are electrons. In this case the Hall coefficient is negative because the electron has a negative charge q. In semiconductors the majority of carriers can also be holes with a positive charge in which case the Hall coefficient is positive [115].

The deflection of the charge carriers not only creates the Hall voltage, it also results in a higher resistance because the carriers take a longer path. This effect is called the magnetoresistive effect [128, 117]. The change in resistance in classical MR sensors is generally only a few percent. Similar to strain gauges and piezoresistive sensors the sensitivity can be enhanced by implementing the MR sensors in a Wheatstone bridge [115]. The choice between Hall and MR sensor depends on the required sensitivity and the possibility of adding two additional electrodes to measure the hall voltage [129].

Among the papers listed in Table 1 two of them are based on Hall sensors. McKinley et al. [87] have proposed a disposable probe to palpate tissue and look for subcutaneous blood vessels in RAMIS.

The spring loaded probe tip is used to move permanent magnets up and down next to a Hall effect encoder. The spring stiffness and the measured displacement are used to determine the applied force. The result is a relatively cheap and simple force sensor [87].

Jones et al. use the Hall effect to measure forces at the tip of a disposable grasper in MIS [86]. To do so they have placed a permanent magnet inside the hard layer of the toothed grasping surface. The magnet is separated from the Hall sensor by a layer of soft silicone rubber. Therefore, when a grip force is applied the magnet moves closer to the Hall sensor proportional to the force. This way the sensor is able to measure the grip force up to 35N as well as shear (x-direction) force up to 7N with [86].

5.4.2 Inductive sensors

A popular inductive sensor suitable for measuring small displacements and forces is called the Linear Variable Differential Transformer (LVDT) [116]. A LVDT consists of three coils and a concentric ferromagnetic core as shown in Figure 14. The middle coil is supplied with an AC voltage resulting in an alternating magnetic field. The other two coils are inductively coupled to the central coil by the core. The induced voltages in the sensing coils are subtracted such that when the core is in the middle position the sensor reads 0V. When the core moves, due to an applied force for example, the induced voltage in one of sensing coils increases and decreases in the other [116, 85].

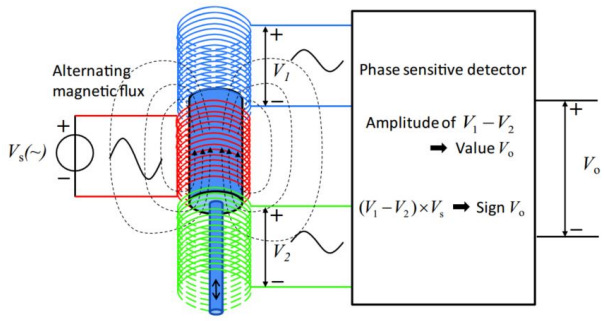

Figure 14: Schematic construction of an LVDT. When the core is in the middle the output is zero. When the core moves the voltage at one coil will increase. Figure adapted from [116].

The LVDT has been used by Darvish et al. to construct a palpation probe for MIS [85]. Similar to the probe proposed by McKinley et al. it uses a spring mounted probe tip. In this case the movement of the probe tip causes a change in position of the ferrite core relative to the three coils. Combined with the spring stiffness this displacement is used to determine the forces up to 3N [85]. While the result is a robust and relatively accurate sensor it could be questioned whether a LVDT can be made small enough, sterilizable, or cheap enough to be disposable.

5.5 Input force sensing

This force sensing strategy does not directly measure the external forces applied to the tip. Instead, it determines the forces the robot generates to move the instrument, close the grasper or steer the tip. These input forces are subsequently used to estimate the corresponding external force at the tip. The lack of distal sensors, or any sensors at all, prevents any concerns about biocompatibility, sterilization, size, reusability or EM interference. Depending on the forces one wants to know there are several ways to implement this strategy .

When the instrument is steerable and cable driven like the one in Figure 1 it is possible to determine the grip force by measuring the tension in the cables that actuate the instrument. The x and y forces can also be measured through the cable driven joints that pitch and yaw the instrument tip. The tension on the cables can be determined by measuring the tension directly [89, 95, 100]. The tension can also be determined by measuring the current going to the actuators that pull on the cables. Since for DC-motors the output torque is linearly related to the current this is a relatively simple calculation. Most of the examples included in Table 1 use cable actuator current and angular position measurements to estimate tip forces [88, 93, 98, 99, 102, 103]. Two of the included examples use pneumatic cylinders to drive the cables that actuate the instrument. So instead of motor current they use changes in cylinder pressures along with position measurements to estimate tip forces. Because they use instruments with different actuation mechanisms they are able to measure forces in more DoF [96, 90]. Matich et al. implemented tip force estimation in an instrument intended for NOTES. Their instrument uses push/pull rods to actuate the instrument. Therefore they measure the tension/compression on the rods at the actuator [94].

Estimating the tip forces through the actuator torque and displacement involves complex dynamic and kinematic equations. Additionally, there are several sources of friction in the system that make the system highly non-linear and more difficult to model accurately. Most of the examples have included friction models in the dynamic model of the system [89, 90, 93, 95, 96, 98, 99, 103]. Others use neural networks with a training data-set to fit a model to the complicated friction effects in the system [101, 102]. Then there are also two examples that use neural networks to model the complete

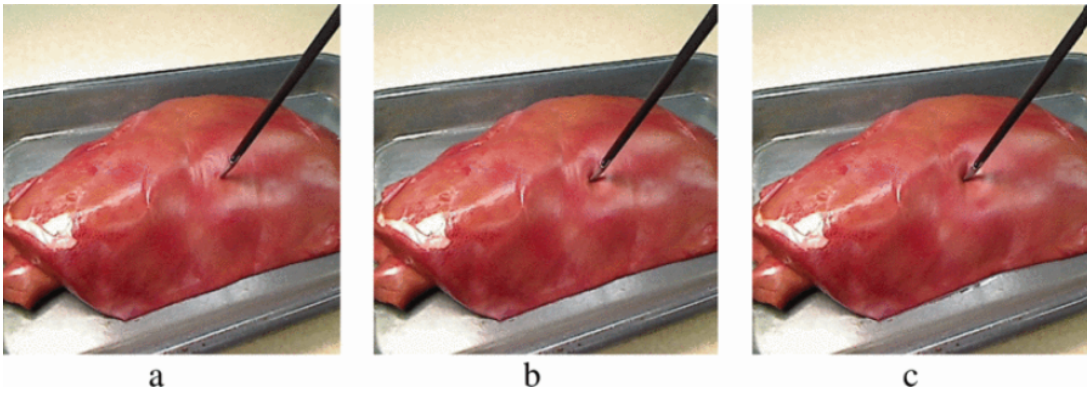

Figure 15: Three images to indicate visual changes resulting from increasing instrument-tissue interaction forces. Figure taken from [110].

system [88, 92]. Matich et al. [94] use a completely different approach. They didn't include friction in the system model nor did they use neural networks to come up with a model. Instead they reduce friction in the system through high frequency vibrations. By doing this they are able to eliminate cross-sensitivity and reduce hysteresis by a factor of 4 [94]. The data included in Table 1 are inconclusive as to which of these approaches results in the highest accuracy.

Two of the examples are able to estimate the x,y and z forces on the conventional cable driven RAMIS instrument tip without the use of sensors. This is achieved by measuring both cable actuator torques and the torques created in the actuators of the robot arm [91, 97]. While this enables the estimation of forces in the z-direction it also further complicates the kinematic equations used to estimate the tip forces. Moreover, this estimation method is influenced by both friction in the instrument and forces occurring at the trocar as explained in Section 3.2.1. The model used by Sang et al. includes a tendon-pulley friction model for the internal friction but does not account for the trocar forces [97].

The force sensing and estimation solution proposed by Yilmaz et al. [101] is able to measure or estimate forces and torques at the instrument tip in 6 DoF. It does so by combining measurements of instrument actuator forces and displacements with measurements from a 6 DoF force sensor mounted at the interface between the instrument and robot arm. This system also uses a dynamic model to relate the measured forces at the interface to force at the tip. The instrument actuator data is related to external forces through a trained neural network model [101]. This hybrid approach to data acquisition and system modelling results in the highest accuracy in this category while measuring in 6 DoF.

All but one of the papers in this category discuss a way in which they account for friction [91]. Nonetheless it must be added that the performance figures in Table 1 are probably still not indicative of real life performance. None of the examples has been tested in an *ex vivo*,*in vivo* or otherwise representative setting. The friction parameters and training data-sets were obtained in dry laboratory settings. This means that the models are likely unable to cope with changing friction characteristics due to moisture or changes of temperature as well as the interaction forces from the trocar and abdomen.

5.6 Image based sensing

Image based estimation methods use images of the surgical field, provided by the endoscope, to estimate the force being applied to a tissue. What is interesting about this approach is that it is able to obtain force data from inside the body without the use of invasive sensors. In most cases the images from the endoscope are used to determine the indentation dept of the instrument in the tissue and from that calculate the corresponding interaction force [104, 106, 107, 109, 110]. Figure 15 shows how an increasing interaction force can clearly be visually recognized. An advantage of this approach is that no equipment is required which is not already used in MIS.

There are multiple ways one could go about the detection of indentation depth and estimation of force. The solutions provided by Aviles et al, Gao et al. and Marban et al. [104, 106, 109] use neural networks and shape recovery algorithms to relate the images to force data. More specifically, Aviles and Marban use a type of recurrent neural network (RNN) called a Long-Short Term Memory (LSTM) network and Gao uses a Temporal Convulutional Network (TCN). The networks are trained with data obtained through images of an instrument interacting with artificial or *ex vivo* tissue. [104, 106, 109]. Marban et al. used a part of the training data to evaluate the performance of

the system after training [109]. Gao et al. used data obtained with a phantom and *ex vivo* tissue separately to train and validate the network and compare the results [106]. Aviles et al. used both a part of the *ex vivo* training data and another set of *in vivo* data obtained with porcine tissue [104]. Table 1 shows that both were able to obtain a high accuracy.

Noohi et al. took a different approach to the detection of indentation depth with endoscope images [110]. Instead of using a neural network they came up with their own force estimation algorithm. The algorithm is based on the assumption that the tissue is a continuously smooth surface (which often the case in the human body) with a local deformation caused by interaction with the instrument. The algorithm compares the smooth surface approximation with the deformed situation in the image. The force is finally estimated using the obtained indentation depth and the stress-strain relation. Experimentation with a lamb liver showed that the algorithm has a relatively low error [110].

A similar method is proposed by Haouchine et al.[107]. Using a depth map obtained through the stereoscopic endoscope images they make a physical 3D reconstruction of the scene through the finite element method. With this reconstruction and by tracking the instrument tip any contact with the tissue can be detected. The contact force is calculated by tracking the tip displacement when in contact [107].

While these three examples of tissue indentation force estimation have achieved good accuracy so far there are still some factors which may complicate their use in practice. First of all there are some effects that can reduce the image quality. The high reflectivity of moist tissues *in vivo* can cause bright spots in the image [104, 110]. Also movement of the endoscope and smoke can reduce the image quality [110]. There are also occlusions which may hide or influence the detection of indentation. These occlusions can be caused by instruments or by fluids like blood [104, 110]. Some of these factors can be mitigated by using stereo vision. This however comes with considerable cost [110]. A final issue is that in some cases the instrument might be puncturing the tissue instead of indenting. This will be particularly difficult to include in the algorithm put forward by Noohi et al. and Haouchine et al. Also the neural network based solutions will have to be trained specifically to detect such events.

The final two examples included in Table 1 both use the images provided by the endoscope in a completely different way from the previous three. Faragasso et al. have provided a means of palpating tissues in MIS using only the endoscope and a disposable add-on [105]. The add-on is placed around the end of the endoscope and has four cantilever beams protruding in front of the lens under an angle as shown in Figure 16. When the endoscope with cantilevers is pushed into the tissue the beams will deflect more into the view of the endoscope. However, the beams not deflect equally because one of the beams has a different stiffness from the other three. The relative deflection of the beams can subsequently be measured through image processing and used to calculate the tissue stiffness [105].

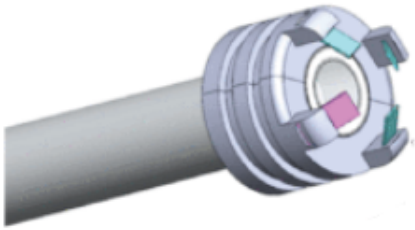

Figure 16: Image based palpation instrument added onto an endoscope. Figure taken from [105].

A similar but reusable strategy was proposed by Watanabe et al. [111]. Their system involves a piece of panty stocking fabric being placed in front of the endoscope. In front of the stocking material is a pin which, when pressed into tissue, deforms the stocking material. The deformation is registered by the endoscope and related to a force through a calibration curve [111].

Maeda et al. have proposed another different approach [108]. Their solution involves deformable structures placed at the instrument tip. The structures consists of a deformable silicon layer which is separated from a transparent glass layer by a small gap. The gap is small enough that light reflected off the silicon layer interferes with the incoming light. As a result only one color of light is reflected back making the structure look green. The color of the reflected light is visible through the endoscope. When a force is applied normal to the deformable silicon layer the size of the gap will change uniformly. The change of gap size will result in a uniform change in color being reflected to be picked up by the endoscope. When a force is applied in a transverse direction the deformable structure will tilt and result in what they call a 'slope of color'. Implementing these structures at the tip will allow for the measurement of grip forces as well as forces in the x- and z-directions. So far however the maximum force of the structure is lower than the expected grip force. There are also no accuracy figures provided in the paper [108].

5.7 Acoustic sensing

The acoustic sensing category is distinguished by the use of sound waves for the measurement of forces. This can be low frequency waves but also high frequency ultrasound waves. Using sound waves instead of electrical signals results in an inherently sterilizable and EM insensitive sensor with very few parts.

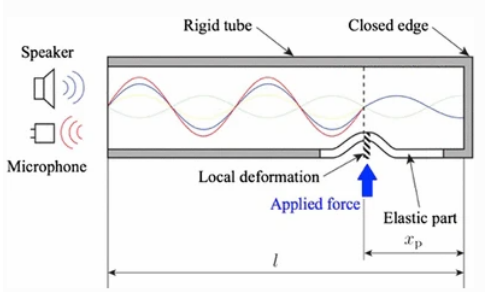

Figure 17: Acoustic reflection sensing principle. Figure taken from [112]

Only one example of acoustic force sensing has been included in Table 1. Ly et al. use a sensing principle based on acoustic reflection [112]. It works by sending a sound wave into an acoustic cavity. At the end of the cavity, at the instrument tip, there is a deformable part of the cavity. When no force is applied the acoustic wave travels through the cavity and reflects only at the end of the cavity. The amplitude of the reflected wave is measured by a microphone at the beginning of the cavity. When a piece of tissue is grasped a force is applied to the deformable part pushing it into the cavity. Now there is not only a reflection occurring at the end of the cavity but also at the deformed region some distance from the end. This is shown in Figure 17. The additional reflection can be detected by a change in amplitude or a phase difference measured by the microphone. The size of the effect provides information on the size of the deformation and thus the force. By implementing two cavities that deform in different directions they were able to create a 2 DoF sensor [112].

The force range and accuracy shown in Table 1 are still inadequate for grasping force measuring in MIS. However, improvements can be made by optimizing the stiffness of the deformable part. Since the wave velocity depends on temperature the sensor is still sensitive to changes in temperature. No solution to this sensitivity was put forward in [112].

5.8 Pressure based sensing

Pressure based force sensors measure changes in pressure caused by an applied force. In Section 5.5 two papers were discussed that use pressure differential in their sensing strategy [96, 130]. However, since this pressure is measured at the actuator to estimate the actuation forces they are not included here. The paper that is included here uses pressure measurements to estimate the external force directly. The way Gaudeni et al. [113] have implemented their sensor it does not measure external forces exerted on the tip. Instead they have integrated a small inflatable structure in the distal shaft of the instrument. When deflated it does not protrude from the shaft. However, when a force measurement is needed it can be inflated, pressed against tissue and used for palpation. The change of pressure when in contact allows for the calculation of the contact force with reasonable accuracy [113].

The proposed sensor has some clear advantages; it does not need electrical connections near the tip and as a result it is insensitive to EM interference. The device is cheap and disposable but with proper material selection could also be sterilizable. By the way in which it is integrated it does not increase the size of the instrument and is not in the way when it is not being used [113]. Pressure sensors with an enclosed volume are however sensitive to changes in temperature. No mitigation measure against this was provided in the paper but including a temperature sensor and using the ideal gas law might already be sufficient.

6 Discussion

Figure 18 shows how the publication dates of the included papers and different categories are distributed. The figure shows that force sensing in MIS has been an increasingly popular topic with 28 papers being published over 2017 and 2018. This rise coincides with the approval and subsequent popularization of robotic surgery.

Not only has the topic become very popular over the past 20 years, it has also become a very diverse field. Figure 18 shows how the included literature is spread over the 8 different sensing categories and over time. It must be noted that the figure might provide a slightly distorted view since only the latest iterations of certain sensors were included. This means that they appear later in time while their first iteration might have been published some years earlier. Nonetheless, it shows that the category which is currently the largest, the resistive sensors, has also been popular for the longest time. Already since 2003 at least one paper using resistive senors has been published almost every year. As the oldest category included in this study the optical sensors have become the much more popular category in the pas two years. Almost all the other categories have mainly gathered interest in the last 5 to 10 years. Therefore they could still catch-up in terms of the number of pa-

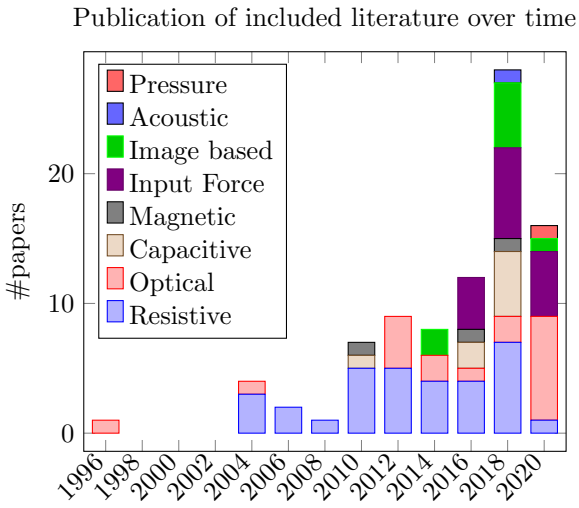

Figure 18: Distribution of included papers and categories over the past 24 years.

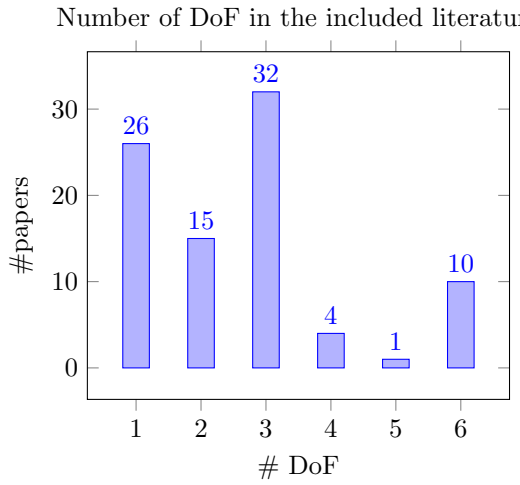

Figure 19: Number of Degrees of Freedom (DoF) in the proposed sensing strategies

pers published. Especially the input force based sensing strategies have recently gained considerable attention.

The number of different sensing strategies and their popularity over time shows that no generally preferred strategy has been found yet. Moreover, within each category there is an even greater diversity of sensor types and solutions. In table 1 and Section 5 it can be seen and read that the solutions can differ greatly in application, specifications, mechanical construction and performance. The large diversity is likely due to the numerous and strict requirements associated with force sensing in MIS. The strict requirements make picking one sensing strategy over another mostly a trade-off between requirements.

The following sections will return to the requirements and considerations put forward in section 3 and discuss how the included literature relate to them. Doing so will exemplify the trade-offs and wide ranging specifications between the proposed solutions.

6.1 Degrees of Freedom

In section 3.1.1 it was explained that the number of DoF one needs to measure depends on the application. For force feedback and force limiting it is not strictly necessary to measure forces in all DoF to obtain useful improvements. For palpation only one DoF might already be sufficient.

Figure 19 shows that for more than 80% of included literature it was decided not to measure all DoF. Most commonly only one or 3 DoF are measured.

Almost all of the 3 DoF strategies measure or estimate the linear forces in the x, y and z directions. Since these forces are perhaps most relevant for improving safety as well as tissue handling it is not surprising that so many examples have chosen to focus on these forces.

Interestingly, the strategies that measure torque around the z-axis are almost all 6 DoF sensors. Only two exceptions propose to measure the torque around the z-axis with a 4 or 5 DoF sensor. None of the references explicitly state why they chose to have a 6 DoF instead of a 4 DoF sensor. Perhaps the torque around the z-axis was not deemed specifically relevant for tissue interaction or suturing after all. It might also be more complicated to design and implement a compliant structure, or sensor arrangement, that allows only this torque to be measured but not the other two torques. Moreover, 6 DoF sensors are more readily available off-the-shelf.

The one DoF group is split between sensing strategies that only measure or estimate the grip force and those that only measure force in the z-direction. On top of the single DoF grip force sensors there are 11 other sensors that have included grip force measurements bringing the total to 25. For 4 of those the grip force is combined with only the x and y linear forces. With cable driven steerable instruments all three of those DoF can be estimated through the cable tension. 5 others measure all three linear forces along with the grip force. Most of these are tip mounted sensors. The relatively high number of grip force sensors reflects the fact that inappropriate grip force is considered one of the most common and interesting error modes during surgery.

The group that only measures forces in the z direction consists mainly of palpation instruments. There are however also 10 palpation instruments that measure forces in 3 or more DoF, one of which measures in 6 DoF.

The 10 included 6 DoF sensors form a quite uniform group. All but one of them are intended for use in RAMIS. This is not surprising considering that with MIS instruments there are only 5 DoF. They also all measure the x,y and z forces and torques, so no grip force.

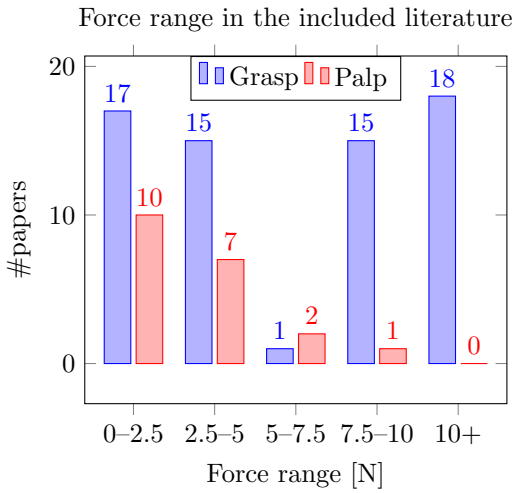

Figure 20: Force ranges of the proposed sensing strategies split between grasper instruments in blue and palpation instruments in red. Note: For multi-DoF sensors the largest range is used.

6.2 Sensing Range

In Section 3.1.2 it was argued that the measurement range should be around 10N for tissue interaction forces and at least 4N for grip forces. For palpation it was found that, although a bit more arbitrary, a range of 2N should suffice. Figure 20 gives an overview of the force ranges for grasping and palpation instruments found in the literature. It shows an almost uniform distribution of force ranges in grasping instruments. Only 26 out of the 64 force sensing strategies in grasping instruments meet the 10N and 4N requirements. For palpation instruments 7 out of 20 have a range greater than or equal to 2N.

A possible explanation for this low 'passing rate' is that due to technical challenges it is difficult to meet these requirements. Especially for distal sensors that have to fit through a narrow trocar a large sensing range can be challenging. Fore some solutions the compliant structure used to separate different force components has only a limited strength due to the lack of space. In other cases the small space reduces the amount of displacement that can be achieved under load. Both factors reduce the maximum measurement range for distal sensors. Many of the proposed sensors also have an axial z-force range that is more than twice as high as the x- and y-forces that act in bending. This is a result of the fact that the strength or stiffness of the instruments is also different in those directions. In both cases increasing or decreasing the strength or displacement range also influences the obtained resolution of the sensor. Therefore the results found in the literature are likely the result of a trade-off between range, resolution and the stiffness in the different directions.

A second explanation for the low 'passing rate' is the lack of information on what the force range during surgery actually is. In Section 3.1.2 it was already discussed that the currently available data for the sensing range were obtained with sensors that were mounted proximally on MIS instruments. This means that the measurements were affected by the distortion effects discussed in Section 3.2.1. To date no distally mounted sensor has been used in a realistic laparoscopic surgical environment in order to obtain force data during a procedure. Therefore there is no data yet of the actual interaction forces that occur during surgery. This means that it is almost impossible to ascertain the exact force range required for force feedback or force limiting.

As mentioned in Section 3.1.2 the sensing range for palpation instruments is somewhat arbitrary. Whether the range is adequate depends mostly on whether the resolution within the range is high enough to differentiate tissue stiffness.

6.3 Location

In Section 3.2.1 the locations at which one could place a sensor were listed. It was explained that the choice of location is a trade-off between the required accuracy and biocompatibility, reusability and size requirements. Figure 21 shows if and where it was decided to include sensors in the literature. Given the accuracy limitations of proximal sensors and estimation methods outlined in Section 3.2.1 it is not surprising to find that almost two-thirds of the examples include sensors placed at distal locations.

Also interesting is that 32 papers propose 'sensorless' or proximal solutions to force estimation. The sensorless solutions include the input force and image based sensing methods that do not require any additional sensors added to the instrument. These solutions as well as the proximal sensors, according to the limitations, should not be able to produce accurate results. Nonetheless, some of the data in Table 1 suggests that these strategies can still be relatively accurate.

There are however some reasons for apprehension when interpreting these results. Firstly, although this category (especially the input force category) includes some examples of relatively accurate estimations it also includes some of the lowest accuracy results.

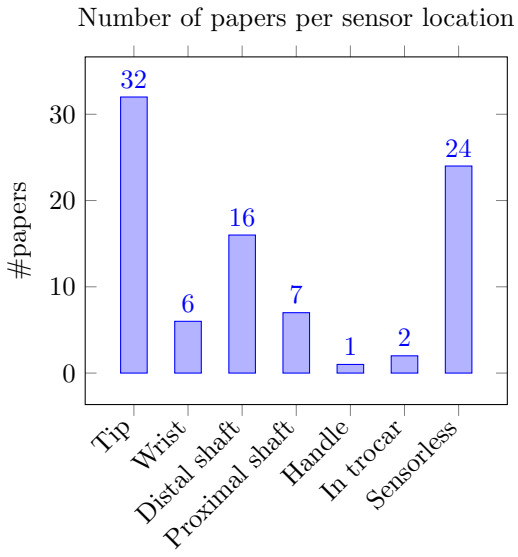

Figure 21: Distribution of relevant papers over the different sensor locations.

A second reason for apprehension is the validation process of these strategies. As stated before, none of the distal sensors that were found for this review have been used in a representative laparoscopic surgical procedure. The same is also true for the proximal and sensorless estimation methods. Most solutions in these categories have only been tested and validated in an experimental setting. Some have also been validated using *ex vivo* organs or tissue phantoms. None of them were validated in a setting close to a true surgical procedure with a trocar, inflated abdomen, blood and other fluids and multiple instruments. This fact is of particular importance because these are precisely the factors that might severely limit the accuracy of proximal or sensorless estimation strategies. For strategies that use proximal shaft sensors or calculate robot arm torques to estimate tip forces the effect of the trocar and inflated abdomen might significantly reduce the accuracy. Strategies that involve the measurement of internal cable tension are not necessarily affected by trocar and abdomen forces. They could however be significantly affected by blood and other fluids that change the internal friction. Moreover, they only work for cable driven steerable instruments which are not the only type of instrument used in RAMIS. The image based strategies are not affected by the trocar and abdomen or by a change of instrument friction. However, the use of flushing fluids, the presence of blood, gauze, or instruments can obstruct the view and reduce the effectiveness of this solution. All of these unknowns show that the current level of validation of these strategies is insufficient to tell whether they have a useful future in this field.

6.4 Performance

There are several factors that make it difficult to give a reliable comparison based on the performance specifications listed in Table 1. Firstly, the categories of Magnetic, Input force, Image based, Acoustic and Pressure based sensing cannot be included because they contain too few usable data points to make a fair comparison with the other categories. Secondly, the included papers use several different measures of error or accuracy (Max error, RMSE, average error). Therefore it is not useful to blindly average the error between categories in order to compare them in terms of accuracy.

Based on the range and resolution specifications some basic comparisons can still be performed. However, since not all papers included data on the sensing range and/or resolution only some entries are usable for comparison. Also significant outliers compared to the other papers were excluded.

The first comparison is performed by looking at just the resolutions as listed in Table 1. First it must be said that out of the 47 papers that provided numbers on the resolution only 9 have resolutions larger than the 0.15N upper limit provided in Section 3.1.3. Comparing the average resolution between the sensor types they rank as follows: 1. Capacitive 2. FBG, 3. Piezoresistor, 4. LIM, 5. Strain gauge. It must be noted however that one outlier (a resolution of 1450 mN) in the capacitive category was excluded.

Since the range and resolution are generally inversely proportional to each other it is also useful to compare the averaged ratio of range divided by resolution of each category. Doing so yields the following ranking: 1. Capacitive, 2. FBG, 3. LIM, 4. Piezoresistor, 5. Strain gauge. Also here an outlier, with an extremely high ratio, in the piezoresistive sensor category was excluded.

This crude performance evaluation suggests that the capacitive sensors provide the best combination of range and resolution. As the results in Table 1 show these sensors are also able to measure forces and torques in 3 or more DoF.

6.5 Bandwidth

In Section 3 it was explained that the human kinesthetic bandwidth is limited to approximately 30Hz. Therefore a minimum sensor bandwidth of 30Hz for force feedback was proposed. It was also noted that when a sensor is included in a control loop (with or without a human controller) a higher bandwidth may be necessary to obtain a stable system.

From the included papers it became clear that the bandwidth or sampling frequency of the sensor was not a major concern. Less than 40% of all papers contained any information on the sensor

bandwidth or sampling frequency. For the papers that do include some numbers on the bandwidth they are generally well above the 30Hz limit. Only three papers say their sampling frequency is under 30Hz and only nine are lower than 100Hz.

The category that is most limited in terms of bandwidth are the image based strategies. These solutions are limited by the sampling rate of the endoscope that is being used. With camera sampling rates often around 30Hz it is difficult to exceed the lower limit. However, when the processed images are used for visual force feedback there might be little need to increase this rate due to the limited human visual bandwidth.

6.6 Reusability and cost

As discussed in Section 3.2.1 for a sensing strategy to be reusable, it has to be sterilizable. While this is not, or hardly, an issue for sensorless and proximal solutions it is a limitation for distal sensors. Out of the more than 50 proposed distal sensors only 24 are claimed to be reusable through sterilization.

For example, while the capacitive sensors provide great sensitivity, none of the papers proposing capacitive sensors state that their solution is reusable. This is likely due to the high sensitivity to EM interference which requires the processing electronics to be placed near the tip. Having the processing electronics near the sensor, also reduces the chance that capacitive sensors will be able to suit 5mm or even 3mm instruments due to the size limitations.

As an exception among the distal sensors, all of the papers describing FBG sensors claim that their solution is reusable. The FBG sensors also benefit from a very small size. The optical fibers that contain the FBG can be smaller than 250μm in diameter and are therefore easily integrated into instruments.

Most of the 24 studies that claim their solution is reusable do so because they use materials and adhesives rated for the required temperature (134°C). There are however only two studies that have actually demonstrated the sterilizability. Trejos et al. found that a strain gauge sensor with optimal material and adhesive choice could be sterilized about 6 but has to be recallibrated after every cycle [40]. The strain gauges mounted on the instrument handle by Fahkry et al. were sterilized 10 times without deterioration [27]. However, since even the semi-reusable instruments used in RAMIS last 16 procedures a lifetime of 6 or 10 sterilization cycles is not sufficiently reusable. The study by Trejos et al. shows that even choosing materials and adhesives with the proper characteristics does not guarantee a reusable and repeatable sensor with a limited error. So for the 23 other studies that claim their sensor is reusable it is still the question whether that will turn out to be the case.

As explained in Section 3 reusability is a matter of being able to both clean and sterilize the sensor. It was discussed that in order to be cleanable, distal sensors should not include small open crevices from which any residue cannot be effectively removed. Similar to sterilizability this is a topic not mentioned in most papers. For those that do claim their sensor is sterilizable it could pose an additional problem. Many sensors include compliant structures to improve the sensitivity and reduce cross-talk. These structures often include small crevices that are difficult to clean. For many sensors it would be possible to fill the crevices with a flexible material to stop residue form accumulating while maintaining the function. However, this is something that should be accounted for in the design stage because of the altered stiffness of the system.

As pointed out in Section 3 the cost of any sensing strategy is a very important consideration. It also further complicates any attempt at pointing out the best or preferred sensing strategy. This is partly due to the fact that the capacitive sensors with the highest sensitivity are not reusable. As explained before, a non reusable sensor means that at least the sensor but likely also the instrument has to be discarded after a single use.

The relatively sensitive and potentially sterilizable FBG sensors appear to be a reasonable alternative. However, the optical interrogators that are required to read out these sensors can cost between €10.000 and €20.000 [131]. Although, recently a lot of research has been published on alternative low-cost interrogators [132]. Nonetheless, it is currently still more expensive than the read-out electronics required with, for example, resistive sensors. Moreover, when applied to limited reusability instruments like those used in RAMIS the FBG sensor and instrument will still have to be replaced after 16 procedures.

The sensors that are perhaps cheapest in terms of interrogation hardware, software and fabrication cost are the resistive sensors. However, the applicability of these sensors is limited by their fragility, sensitivity and the fact that their are only sterilizable a few times, if at all.

Finally, it has to be acknowledged that the input force and image based categories include infinitely reusable solutions. Since they are (mostly) software based solutions the initial investment is also limited. However, as mentioned before, it is still the question whether these strategies will work in practice.

7 Conclusion

In the introductory sections of this review it was discussed that there are several reasons and applications for force sensing in MIS. It is possible to use force measurements for palpation to find tumors or blood vessels, for force limiting to prevent accidental tissue damage, or for force feedback to improve tissue handling and safety.

In the section that followed the requirements associated with these applications and force sensing in MIS in general were explored. Although there are some particularly strict requirements it became clear that not all of them are narrowly defined. This means that there is a lot of room for interpretation, preference and trade-offs between different requirements.

The central part of this review focused on the state-of-the-art in force sensing strategies for MIS. The literature collected for this review shows that a great variation of attempts have already been made at sensing forces in MIS. Proposed solutions are spread over several sensing categories and even within categories there is a significant variety.

The analysis of the state-of-the-art has provided some interesting insights on how the trade-offs between requirements and sensing strategies have turned out. It showed that more than 80% of the proposed solutions did not measure or estimate forces in all the available DoF. Instead, most implemented 1 or 3 DoF sensors focusing on the grip force or x-y-z forces. A similar distribution was observed for the sensor location. More than two-thirds of all solutions used a sensor placed at distal locations. Interestingly, 32 solutions use proximal or sensorless solutions, regardless of the accuracy limitations often associated with these strategies. Some of the sensorless and proximal solutions even appear to be relatively accurate. However, none of these solutions were validated in a manner that is sufficiently representative to actually show the accuracy limitations.

For some of the requirements there appears to be even less consensus on their interpretation and importance. For example only 24 out of more than 50 listed distal sensors are supposed to be sterilizable and thus reusable. Moreover, only two studies have verified whether and to what extent their sensor is reusable. Also for the sensing range little coherence was found. For grasper instruments the proposed sensing ranges are spread almost uniformly between 1 and more than 10N. Possible explanations for this are technical limitations and a lack of exact and reliable measurements of the actual required range.

In trying to point out which sensing strategy might be the best based on the included literature one is confronted with several limitations, a wide variety and a lack of sufficient validation. Based on a basic evaluation of the performance figures the capacitive sensors would appear the best solution. However, these sensors, with local electronics, are relatively large and none of these sensors is reusable at this time. The sensor type for which all papers claim that the sensor is reusable is also the second best in terms of sensitivity. However, none of the proposed FBG sensors have actually been tested to be sterilizable and repeatable. The FBG sensors also rank as the most expensive sensing strategy with current interrogator technology. Sensors that are relatively cheap, in terms of sensor and processing hardware cost, are the resistive sensors (strain gauges and piezoresistors). The low cost might be necessary considering that they are currently reusable for at most 6-10 times. They also rank as the least sensitive in the basic evaluation performed in this work. Finally, there are the input force and image based strategies which are not limited by size, reusability or cost. However, considering the aforementioned lack of validation, it is not yet possible to say whether they will turn out to be sufficiently accurate for any practical application.

In conclusion, much work has already been published on force sensing in MIS. However, a lot of uncertainty still remains with regard to the actual required sensing range, reusability and real-life performance of the proposed solutions. As a result, determining the best solution is still mostly a matter of trade-offs and interpretation specific to each application.

Much of the uncertainty and division in this field can be attributed to a lack of sufficiently representative validation. Therefore more research is required to fill these gaps. This could include the use of a tip mounted force sensor to obtain (more) reliable force range data. For example through a cadaver surgery study. It is also important that the performance and particularly the accuracy of sensorless and proximal solutions are investigated in a realistic setting. This could be performed with a validated tip mounted sensor along with sensorless or proximal sensors during actual surgery or a cadaver surgery. Alternatively one could design and build a phantom abdomen and fit it with a trocar to find its influence in a more experimental setting. Finally, the reusability and repeatability of most of the sensor types needs to be verified. Especially the autoclave sterilization is relevant here.

References

[1] P. Puangmali, K. Althoefer, L. D. Seneviratne, D. Murphy, and P. Dasgupta, "State-of-the-art in force and tactile sensing for minimally invasive surgery," *IEEE Sensors Journal*, vol. 8, no. 4, pp. 371–381, 2008.

[2] A. Trejos, R. Patel, and M. Naish, "Force sensing and its application in minimally invasive surgery and therapy: a survey," *Proceedings of the Institution of Mechanical Engineers, Part C: Journal of Mechanical Engineering Science*, vol. 224, no. 7, pp. 1435–1454, 2010.

[3] E. P. Westebring-van der Putten, M. C. Berben, R. H. Goossens, J. J. Jakimowicz, and J. Dankelman, "The opinion and experience of surgeons with laparoscopic bowel grasper haptics," vol. 60, p. 28, 2010.

[4] C. Freschi, V. Ferrari, F. Melfi, M. Ferrari, F. Mosca, and A. Cuschieri, "Technical review of the da vinci surgical telemanipulator," *The International Journal of Medical Robotics and Computer Assisted Surgery*, vol. 9, no. 4, pp. 396–406, 2013.

[5] S. F. Hardon, F. Schilder, J. Bonjer, J. Dankelman, and T. Horeman, "A new modular mechanism that allows full detachability and cleaning of steerable laparoscopic instruments," *Surgical endoscopy*, vol. 33, no. 10, pp. 3484–3493, 2019.

[6] S. Rodrigues, T. Horeman, P. Sam, J. Dankelman, J. Van den Dobbelsteen, and F. Jansen, "Influence of visual force feedback on tissue handling in minimally invasive surgery," *Br J Surg*, vol. 101, no. 13, pp. 1766–1773, 2014.

[7] C. E. Reiley, T. Akinbiyi, D. Burschka, D. C. Chang, A. M. Okamura, and D. D. Yuh, "Effects of visual force feedback on robot-assisted surgical task performance," *The Journal of thoracic and cardiovascular surgery*, vol. 135, no. 1, pp. 196–202, 2008.

[8] C. R. Wottawa, B. Genovese, B. N. Nowroozi, S. D. Hart, J. W. Bisley, W. S. Grundfest, and E. P. Dutson, "Evaluating tactile feedback in robotic surgery for potential clinical application using an animal model," *Surgical endoscopy*, vol. 30, no. 8, pp. 3198–3209, 2016.

[9] C.-H. King, M. O. Culjat, M. L. Franco, C. E. Lewis, E. P. Dutson, W. S. Grundfest, and J. W. Bisley, "Tactile feedback induces reduced grasping force in robot-assisted surgery," *IEEE transactions on haptics*, vol. 2, no. 2, pp. 103–110, 2009.

[10] A. Abiri, J. Pensa, A. Tao, J. Ma, Y.-Y. Juo, S. J. Askari, J. Bisley, J. Rosen, E. P. Dutson, and W. S. Grundfest, "Multi-modal haptic feedback for grip force reduction in robotic surgery," *Scientific reports*, vol. 9, no. 1, pp. 1–10, 2019.

[11] G. L. McCreery, A. L. Trejos, M. D. Naish, R. V. Patel, and R. A. Malthaner, "Feasibility of locating tumours in lung via kinaesthetic feedback," *The International Journal of Medical Robotics and Computer Assisted Surgery*, vol. 4, no. 1, pp. 58–68, 2008.

[12] J. Konstantinova, A. Jiang, K. Althoefer, P. Dasgupta, and T. Nanayakkara, "Implementation of tactile sensing for palpation in robot-assisted minimally invasive surgery: A review," *IEEE Sensors Journal*, vol. 14, no. 8, pp. 2490–2501, 2014.

[13] M. I. Tiwana, S. J. Redmond, and N. H. Lovell, "A review of tactile sensing technologies with applications in biomedical engineering," *Sensors and Actuators A: physical*, vol. 179, pp. 17–31, 2012.

[14] B. Tang, G. Hanna, P. Joice, and A. Cuschieri, "Identification and categorization of technical errors by observational clinical human reliability assessment (ochra) during laparoscopic cholecystectomy," *Archives of surgery*, vol. 139, no. 11, pp. 1215–1220, 2004.

[15] E. Heijnsdijk, H. De Visser, J. Dankelman, and D. Gouma, "Slip and damage properties of jaws of laparoscopic graspers," *Surgical Endoscopy and Other Interventional Techniques*, vol. 18, no. 6, pp. 974–979, 2004.

[16] E. P. Westebring-van der Putten, R. H. Goossens, J. J. Jakimowicz, and J. Dankelman, "Haptics in minimally invasive surgery–a review," *Minimally Invasive Therapy & Allied Technologies*, vol. 17, no. 1, pp. 3–16, 2008.

[17] L. N. Verner, K. A. Jeung, and A. M. Okamura, "15 effects of gripping and translational forces on teleoperation," in *Multi-point Interaction with Real and Virtual Objects*, pp. 231–241, Springer, 2005.

[18] G. Picod, A. Jambon, D. Vinatier, and P. Dubois, "What can the operator actually feel when performing a laparoscopy?,"

Surgical Endoscopy and Other Interventional Techniques, vol. 19, no. 1, pp. 95–100, 2005.

[19] L. Toledo, D. Gossot, S. Fritsch, Y. Revillon, and C. Reboulet, "Study of sustained forces and the working space of endoscopic surgery instruments," in *Annales de chirurgie*, vol. 53, p. 587, 1999.

[20] X.-D. Yang, W. F. Bischof, and P. Boulanger, "Perception of haptic force magnitude during hand movements," in *2008 IEEE International Conference on Robotics and Automation*, pp. 2061–2066, 2008.

[21] H. Pongrac, P. Hinterseer, J. Kammerl, E. Steinbach, B. Färber, U. Muenchen, and T. Muenchen, "Limitations of human 3d force discrimination," *Human-Centered Robotics Systems*, 2006.

[22] J. Westwood *et al.*, "Quantifying surgeon grasping mechanics in laparoscopy using the blue dragon system," *Medicine Meets Virtual Reality 12: Building a Better You: the Next Tools for Medical Education, Diagnosis, and Care*, vol. 98, p. 34, 2004.

[23] T. L. Brooks, "Telerobotic response requirements," in *1990 IEEE International Conference on Systems, Man, and Cybernetics Conference Proceedings*, pp. 113–120, 1990.

[24] P. Rizun, D. Gunn, B. Cox, and G. Sutherland, "Mechatronic design of haptic forceps for robotic surgery," *The International Journal of Medical Robotics and Computer Assisted Surgery*, vol. 2, no. 4, pp. 341–349, 2006.

[25] W. Sjoerdsma, J. Herder, M. Horward, A. Jansen, J. Bannenberg, and C. Grimbergen, "Force transmission of laparoscopic grasping instruments," *Minimally Invasive Therapy & Allied Technologies*, vol. 6, no. 4, pp. 274–278, 1997.

[26] M. M. Dalvand, S. Nahavandi, M. Fielding, J. Mullins, Z. Najdovski, and R. D. Howe, "Modular instrument for a haptically-enabled robotic surgical system (herosurg)," *IEEE access*, vol. 6, pp. 31974–31982, 2018.

[27] M. Fakhry, F. Bello, G. B. Hanna, *et al.*, "A real-time compliance mapping system using standard endoscopic surgical forceps," *IEEE Transactions on Biomedical Engineering*, vol. 56, no. 4, pp. 1245–1253, 2009.

[28] J. B. Gafford, S. B. Kesner, A. Degirmenci, R. J. Wood, R. D. Howe, and C. J. Walsh, "A monolithic approach to fabricating low-cost, millimeter-scale multi-axis force sensors for minimally-invasive surgery," in *2014 IEEE International Conference on Robotics and Automation (ICRA)*, pp. 1419–1425, 2014.

[29] J. B. Gafford, S. B. Kesner, R. J. Wood, and C. J. Walsh, "Force-sensing surgical grasper enabled by pop-up book mems," in *2013 IEEE/RSJ International Conference on Intelligent Robots and Systems*, pp. 2552–2558, 2013.

[30] C. He, S. Wang, H. Sang, J. Li, and L. Zhang, "Force sensing of multiple-dof cable-driven instruments for minimally invasive robotic surgery," *The International Journal of Medical Robotics and Computer Assisted Surgery*, vol. 10, no. 3, pp. 314–324, 2014.

[31] M. B. Hong and Y.-H. Jo, "Design and evaluation of 2-dof compliant forceps with force-sensing capability for minimally invasive robot surgery," *IEEE Transactions on Robotics*, vol. 28, no. 4, pp. 932–941, 2012.

[32] B. Kübler, U. Seibold, and G. Hirzinger, "Development of actuated and sensor integrated forceps for minimally invasive robotic surger," *The International Journal of Medical Robotics and Computer Assisted Surgery*, vol. 1, no. 3, pp. 96–107, 2005.

[33] K. Li, B. Pan, J. Zhan, W. Gao, Y. Fu, and S. Wang, "Design and performance evaluation of a 3-axis force sensor for mis palpation," *Sensor Review*, 2015.

[34] K. Li, B. Pan, F. Zhang, W. Gao, Y. Fu, and S. Wang, "A novel 4-dof surgical instrument with modular joints and 6-axis force sensing capability," *The International Journal of Medical Robotics and Computer Assisted Surgery*, vol. 13, no. 1, p. e1751, 2017.

[35] S. K. Prasad, M. Kitagawa, G. S. Fischer, J. Zand, M. A. Talamini, R. H. Taylor, and A. M. Okamura, "A modular 2-dof force-sensing instrument for laparoscopic surgery," in *International Conference on Medical Image Computing and Computer-Assisted Intervention*, pp. 279–286, Springer, 2003.

[36] A. Srivastava, R. Xu, A. Escoto, C. Ward, and R. V. Patel, "Design of an ultra thin strain sensor using superelastic nitinol for applications in minimally invasive surgery," in *2016 IEEE International Conference on Advanced Intelligent Mechatronics (AIM)*, pp. 794–799, 2016.

[37] M. Stephan, G. Rognini, A. Sengul, R. Beira, L. Santos-Carreras, and H. Bleuler, "Modeling and design of a gripper for a robotic surgical system integrating force sensing capabilities in 4 dof," in *ICCAS 2010*, pp. 361–365, 2010.

[38] M. Tavakoli, R. Patel, and M. Moallem, "Haptic interaction in robot-assisted endoscopic surgery: a sensorized end-effector," *The International Journal of Medical Robotics and Computer Assisted Surgery*, vol. 1, no. 2, pp. 53–63, 2005.

[39] A. L. Trejos, S. Jayaraman, R. V. Patel, M. D. Naish, and C. M. Schlachta, "Force sensing in natural orifice transluminal endoscopic surgery," *Surgical endoscopy*, vol. 25, no. 1, pp. 186–192, 2011.

[40] A. L. Trejos, A. Escoto, M. D. Naish, and R. V. Patel, "Design and evaluation of a sterilizable force sensing instrument for minimally invasive surgery," *IEEE Sensors Journal*, vol. 17, no. 13, pp. 3983–3993, 2017.

[41] J. Wee, M. Kang, P. Francis, R. Brooks, L. Masotti, D. Villavicencio, T. Looi, G. Azzie, J. Drake, and J. T. Gerstle, "Novel force-sensing system for minimally invasive surgical instruments," in *2017 39th Annual International Conference of the IEEE Engineering in Medicine and Biology Society (EMBC)*, pp. 4447–4450, 2017.

[42] H. Yu, J. Jiang, L. Xie, L. Liu, Y. Shi, and P. Cai, "Design and static calibration of a six-dimensional force/torque sensor for minimally invasive surgery," *Minimally Invasive Therapy & Allied Technologies*, vol. 23, no. 3, pp. 136–143, 2014.

[43] L. Yu, Y. Yan, X. Yu, and Y. Xia, "Design and realization of forceps with 3-d force sensing capability for robot-assisted surgical system," *IEEE Sensors Journal*, vol. 18, no. 21, pp. 8924–8932, 2018.

[44] C. Zheng, Z. Qian, K. Zhou, H. Liu, D. Lv, and W. Zhang, "A novel sensor for real-time measurement of force and torque of colonoscope," in *IECON 2017-43rd Annual Conference of the IEEE Industrial Electronics Society*, pp. 3265–3269, 2017.

[45] F. Anderson, D. W. Birch, P. Boulanger, and W. F. Bischof, "Sensor fusion for laparoscopic surgery skill acquisition," *Computer Aided Surgery*, vol. 17, no. 6, pp. 269–283, 2012.

[46] P. Baki, G. Székely, and G. Kósa, "Miniature tri-axial force sensor for feedback in minimally invasive surgery," in *2012 4th IEEE RAS & EMBS International Conference on Biomedical Robotics and Biomechatronics (BioRob)*, pp. 805–810, 2012.

[47] J. Dargahi and S. Najarian, "An integrated force-position tactile sensor for improving diagnostic and therapeutic endoscopic surgery," *Bio-medical materials and engineering*, vol. 14, no. 2, pp. 151–166, 2004.

[48] Y. Hu, R. B. Katragadda, H. Tu, Q. Zheng, Y. Li, and Y. Xu, "Bioinspired 3-d tactile sensor for minimally invasive surgery," *Journal of microelectromechanical systems*, vol. 19, no. 6, pp. 1400–1408, 2010.

[49] W. T. Latt, T. P. Chang, A. Di Marco, P. Pratt, K.-W. Kwok, J. Clark, and G.-Z. Yang, "A hand-held instrument for in vivo probe-based confocal laser endomicroscopy during minimally invasive surgery," in *2012 IEEE/RSJ International Conference on Intelligent Robots and Systems*, pp. 1982–1987, 2012.

[50] Y. Okuda, A. Nakai, T. Sato, M. Kurata, I. Shimoyama, T. Oda, and N. Ohkohci, "New device with force sensors for laparoscopic liver resection–investigation of grip force and histological damage," *Minimally Invasive Therapy & Allied Technologies*, pp. 1–6, 2020.

[51] J. Radó, C. Dücső, P. Földesy, G. Szebényi, Z. Nawrat, K. Rohr, and P. Fürjes, "3d force sensors for laparoscopic surgery tool," *Microsystem Technologies*, vol. 24, no. 1, pp. 519–525, 2018.

[52] W. Schwalb, B. Shirinzadeh, and J. Smith, "A force-sensing surgical tool with a proximally located force/torque sensor," *The International Journal of Medical Robotics and Computer Assisted Surgery*, vol. 13, no. 1, p. e1737, 2017.

[53] G. Tholey, A. Pillarisetti, and J. P. Desai, "On-site three dimensional force sensing capability in a laparoscopic grasper," *Industrial Robot: An International Journal*, 2004.

[54] P. Valdastri, S. Roccella, L. Beccai, E. Cattin, A. Menciassi, M. Carrozza, and P. Dario, "Characterization of a novel hybrid silicon three-axial force sensor," *Sensors and Actuators A: Physical*, vol. 123, pp. 249–257, 2005.

[55] W. Wang, Y. Zhao, and Q. Lin, "An integrated mems tactile tri-axial micro-force

probe sensor for minimally invasive surgery," in *2009 IEEE 3rd International Conference on Nano/Molecular Medicine and Engineering*, pp. 71–76, 2009.

[56] N. Zemiti, G. Morel, T. Ortmaier, and N. Bonnet, "Mechatronic design of a new robot for force control in minimally invasive surgery," *IEEE/ASME Transactions On Mechatronics*, vol. 12, no. 2, pp. 143–153, 2007.

[57] L. Li, B. Yu, C. Yang, P. Vagdargi, R. A. Srivatsan, and H. Choset, "Development of an inexpensive tri-axial force sensor for minimally invasive surgery," in *2017 IEEE/RSJ International Conference on Intelligent Robots and Systems (IROS)*, pp. 906–913, 2017.

[58] Y. Dai, A. Abiri, S. Liu, O. Paydar, H. Sohn, E. P. Dutson, W. S. Grundfest, and R. N. Candler, "Grasper integrated tri-axial force sensor system for robotic minimally invasive surgery," in *2017 39th Annual International Conference of the IEEE Engineering in Medicine and Biology Society (EMBC)*, pp. 3936–3939, 2017.

[59] U. Kim, D.-H. Lee, W. J. Yoon, B. Hannaford, and H. R. Choi, "Force sensor integrated surgical forceps for minimally invasive robotic surgery," *IEEE Transactions on Robotics*, vol. 31, no. 5, pp. 1214–1224, 2015.

[60] U. Kim, Y. B. Kim, D.-Y. Seok, J. So, and H. R. Choi, "A surgical palpation probe with 6-axis force/torque sensing capability for minimally invasive surgery," *IEEE Transactions on Industrial Electronics*, vol. 65, no. 3, pp. 2755–2765, 2017.

[61] U. Kim, Y. B. Kim, J. So, D.-Y. Seok, and H. R. Choi, "Sensorized surgical forceps for robotic-assisted minimally invasive surgery," *IEEE Transactions on Industrial Electronics*, vol. 65, no. 12, pp. 9604–9613, 2018.

[62] D.-H. Lee, U. Kim, T. Gulrez, W. J. Yoon, B. Hannaford, and H. R. Choi, "A laparoscopic grasping tool with force sensing capability," *IEEE/ASME Transactions on Mechatronics*, vol. 21, no. 1, pp. 130–141, 2015.

[63] T. Nagatomo and N. Miki, "Three-axis capacitive force sensor with liquid metal electrodes for endoscopic palpation," *Micro & Nano Letters*, vol. 12, no. 8, pp. 564–568, 2017.

[64] T. Nakadegawa, H. Ishizuka, and N. Miki, "Three-axis scanning force sensor with liquid metal electrodes," *Sensors and Actuators A: Physical*, vol. 264, pp. 260–267, 2017.

[65] P. Peng, A. Sezen, R. Rajamani, and A. Erdman, "Novel mems stiffness sensor for in-vivo tissue characterization measurement," in *2009 Annual International Conference of the IEEE Engineering in Medicine and Biology Society*, pp. 6640–6643, 2009.

[66] N. Bandari, J. Dargahi, and M. Packirisamy, "Miniaturized optical force sensor for minimally invasive surgery with learning-based nonlinear calibration," *IEEE Sensors Journal*, vol. 20, no. 7, pp. 3579–3592, 2019.

[67] S. Ehrampoosh, M. Dave, M. A. Kia, C. Rablau, and M. H. Zadeh, "Providing haptic feedback in robot-assisted minimally invasive surgery: A direct optical force-sensing solution for haptic rendering of deformable bodies," *Computer Aided Surgery*, vol. 18, no. 5-6, pp. 129–141, 2013.

[68] G. A. Fontanelli, L. R. Buonocore, F. Ficuciello, L. Villani, and B. Siciliano, "An external force sensing system for minimally invasive robotic surgery," *IEEE/ASME Transactions on Mechatronics*, vol. 25, no. 3, pp. 1543–1554, 2020.

[69] A. H. H. Hosseinabadi, M. Honarvar, and S. E. Salcudean, "Optical force sensing in minimally invasive robotic surgery," in *2019 International Conference on Robotics and Automation (ICRA)*, pp. 4033–4039, IEEE, 2019.

[70] M. Lazeroms, G. Villavicencio, W. Jongkind, and G. Honderd, "Optical fibre force sensor for minimal-invasive-surgery grasping instruments," in *Proceedings of 18th Annual International Conference of the IEEE Engineering in Medicine and Biology Society*, vol. 1, pp. 234–235, 1996.

[71] H. Liu, J. Li, X. Song, L. D. Seneviratne, and K. Althoefer, "Rolling indentation probe for tissue abnormality identification during minimally invasive surgery," *IEEE Transactions on Robotics*, vol. 27, no. 3, pp. 450–460, 2011.

[72] Y. Noh, S. Han, P. Gawenda, W. Li, S. Sareh, and K. Rhode, "A contact force sensor based on s-shaped beams and optoelectronic sensors for flexible manipulators for minimally invasive surgery (mis)," *IEEE Sensors Journal*, vol. 20, no. 7, pp. 3487–3495, 2019.

[73] J. Peirs, J. Clijnen, D. Reynaerts, H. Van Brussel, P. Herijgers, B. Corteville, and S. Boone, "A micro optical force sensor for force feedback during minimally invasive robotic surgery," *Sensors and Actuators A: Physical*, vol. 115, no. 2-3, pp. 447–455, 2004.

[74] P. Puangmali, H. Liu, L. D. Seneviratne, P. Dasgupta, and K. Althoefer, "Miniature 3-axis distal force sensor for minimally invasive surgical palpation," *Ieee/Asme Transactions On Mechatronics*, vol. 17, no. 4, pp. 646–656, 2011.

[75] H. Choi, Y. Lim, and J. Kim, "Three-axis force sensor with fiber bragg grating," in *2017 39th Annual International Conference of the IEEE Engineering in Medicine and Biology Society (EMBC)*, pp. 3940–3943, 2017.

[76] R. Haslinger, P. Leyendecker, and U. Seibold, "A fiberoptic force-torque-sensor for minimally invasive robotic surgery," in *2013 IEEE international conference on robotics and automation*, pp. 4390–4395, 2013.

[77] W. Lai, L. Cao, R. X. Tan, Y. C. Tan, X. Li, P. T. Phan, A. M. H. Tiong, S. C. Tjin, and S. J. Phee, "An integrated sensor-model approach for haptic feedback of flexible endoscopic robots," *Annals of Biomedical Engineering*, vol. 48, no. 1, pp. 342–356, 2020.

[78] T. Li, A. Pan, and H. Ren, "Reaction force mapping by 3-axis tactile sensing with arbitrary angles for tissue hard-inclusion localization," *IEEE Transactions on Biomedical Engineering*, 2020.

[79] C. Lv, S. Wang, and C. Shi, "A high-precision and miniature fiber bragg grating-based force sensor for tissue palpation during minimally invasive surgery," *Annals of Biomedical Engineering*, vol. 48, no. 2, pp. 669–681, 2020.

[80] K. S. Shahzada, A. Yurkewich, R. Xu, and R. V. Patel, "Sensorization of a surgical robotic instrument for force sensing," in *Optical Fibers and Sensors for Medical Diagnostics and Treatment Applications XVI*, vol. 9702, p. 97020U, International Society for Optics and Photonics, 2016.

[81] C. Shi, M. Li, C. Lv, J. Li, and S. Wang, "A high-sensitivity fiber bragg grating-based distal force sensor for laparoscopic surgery," *IEEE Sensors Journal*, vol. 20, no. 5, pp. 2467–2475, 2019.

[82] H. Song, H. Kim, J. Jeong, and J. Lee, "Development of fbg sensor system for force-feedback in minimally invasive robotic surgery," in *2011 Fifth International Conference on Sensing Technology*, pp. 16–20, IEEE, 2011.

[83] D. S. Yurkewich, A. Escoto, A. L. Trejos, M.-E. LeBel, R. V. Patel, and M. D. Naish, "Low-cost force-sensing arthroscopic tool using threaded fiber bragg grating sensors," in *5th IEEE RAS/EMBS International Conference on Biomedical Robotics and Biomechatronics*, pp. 28–33, 2014.

[84] P. S. Zarrin, A. Escoto, R. Xu, R. V. Patel, M. D. Naish, and A. L. Trejos, "Development of a 2-dof sensorized surgical grasper for grasping and axial force measurements," *IEEE Sensors Journal*, vol. 18, no. 7, pp. 2816–2826, 2018.

[85] B. Darvish, S. Najarian, E. Shirzad, and R. Khodambashi, "A novel tactile force probe for tissue stiffness classification," *arXiv*, 2018.

[86] D. Jones, H. Wang, A. Alazmani, and P. R. Culmer, "A soft multi-axial force sensor to assess tissue properties in realtime," in *2017 IEEE/RSJ International Conference on Intelligent Robots and Systems (IROS)*, pp. 5738–5743, 2017.

[87] S. McKinley, A. Garg, S. Sen, R. Kapadia, A. Murali, K. Nichols, S. Lim, S. Patil, P. Abbeel, A. M. Okamura, *et al.*, "A single-use haptic palpation probe for locating subcutaneous blood vessels in robot-assisted minimally invasive surgery," in *2015 IEEE International Conference on Automation Science and Engineering (CASE)*, pp. 1151–1158, 2015.

[88] Y. Guo, B. Pan, Y. Fu, and M. Q.-H. Meng, "Grip force perception based on daenn for minimally invasive surgery robot," in *2019 IEEE International Conference on Robotics and Biomimetics (ROBIO)*, pp. 1216–1221, 2019.

[89] M. Haghighipanah, M. Miyasaka, and B. Hannaford, "Utilizing elasticity of cable-driven surgical robot to estimate cable tension and external force," *IEEE Robotics and Automation Letters*, vol. 2, no. 3, pp. 1593–1600, 2017.

[90] D. Haraguchi, T. Kanno, K. Tadano, and K. Kawashima, "A pneumatically driven surgical manipulator with a flexible distal

joint capable of force sensing," *IEEE/ASME Transactions on Mechatronics*, vol. 20, no. 6, pp. 2950–2961, 2015.

[91] T. Kasai, D. Nagao, Y. Kuroda, A. Miyamoto, Y. Matsuda, and T. Fukushima, "User interface of force-controlled arm for endoscopic surgery," in *2017 IEEE/RSJ International Conference on Intelligent Robots and Systems (IROS)*, pp. 6477–6483, 2017.

[92] X. Li, L. Cao, A. M. H. Tiong, P. T. Phan, and S. J. Phee, "Distal-end force prediction of tendon-sheath mechanisms for flexible endoscopic surgical robots using deep learning," *Mechanism and Machine Theory*, vol. 134, pp. 323–337, 2019.

[93] Y. Li, M. Miyasaka, M. Haghighipanah, L. Cheng, and B. Hannaford, "Dynamic modeling of cable driven elongated surgical instruments for sensorless grip force estimation," in *2016 IEEE international conference on robotics and automation (ICRA)*, pp. 4128–4134, 2016.

[94] S. Matich, C. Neupert, A. Kirschniak, H. F. Schlaak, and P. Pott, "3-d force measurement using single axis force sensors in a new single port parallel kinematics surgical manipulator," in *2016 IEEE/RSJ International Conference on Intelligent Robots and Systems (IROS)*, pp. 3665–3670, 2016.

[95] K. Miyashita, T. O. Vrielink, and G. Mylonas, "A cable-driven parallel manipulator with force sensing capabilities for high-accuracy tissue endomicroscopy," *International journal of computer assisted radiology and surgery*, vol. 13, no. 5, pp. 659–669, 2018.

[96] R. Miyazaki, T. Kanno, and K. Kawashima, "Pneumatically driven surgical instrument capable of estimating translational force and grasping force," *The International Journal of Medical Robotics and Computer Assisted Surgery*, vol. 15, no. 3, p. e1983, 2019.

[97] H. Sang, J. Yun, R. Monfaredi, E. Wilson, H. Fooladi, and K. Cleary, "External force estimation and implementation in robotically assisted minimally invasive surgery," *The International Journal of Medical Robotics and Computer Assisted Surgery*, vol. 13, no. 2, p. e1824, 2017.

[98] W. Wang, L. Yu, and J. Yang, "Toward force detection of a cable-driven micromanipulator for a surgical robot based on disturbance observer," *Mechanical Sciences*, vol. 8, no. 2, p. 323, 2017.

[99] X. Xin, X. Chen, S. Liu, B. Zhao, P. Gao, Y. Hu, and G. Lv, "Model-based grasp force estimation for minimally invasive surgery," in *2017 IEEE International Conference on Information and Automation (ICIA)*, pp. 489–493, 2017.

[100] R. Xue, Z. Du, Z. Yan, and B. Ren, "An estimation method of grasping force for laparoscope surgical robot based on the model of a cable-pulley system," *Mechanism and Machine Theory*, vol. 134, pp. 440–454, 2019.

[101] N. Yilmaz, M. Bazman, A. Alassi, B. Gur, and U. Tumerdem, "6-axis hybrid sensing and estimation of tip forces/torques on a hyper-redundant robotic surgical instrument," in *2019 IEEE/RSJ International Conference on Intelligent Robots and Systems (IROS)*, pp. 2990–2997, 2019.

[102] L. Yu, W. Wang, and F. Zhang, "External force sensing based on cable tension changes in minimally invasive surgical micromanipulators," *IEEE Access*, vol. 6, pp. 5362–5373, 2018.

[103] B. Zhao and C. A. Nelson, "Sensorless force sensing for minimally invasive surgery," *Journal of medical devices*, vol. 9, no. 4, 2015.

[104] A. I. Aviles, S. M. Alsaleh, J. K. Hahn, and A. Casals, "Towards retrieving force feedback in robotic-assisted surgery: A supervised neuro-recurrent-vision approach," *IEEE transactions on haptics*, vol. 10, no. 3, pp. 431–443, 2016.

[105] A. Faragasso, J. Bimbo, A. Yamashita, and H. Asama, "Disposable stiffness sensor for endoscopic examination," in *2018 40th Annual International Conference of the IEEE Engineering in Medicine and Biology Society (EMBC)*, pp. 4309–4312, 2018.

[106] C. Gao, X. Liu, M. Peven, M. Unberath, and A. Reiter, "Learning to see forces: Surgical force prediction with rgb-point cloud temporal convolutional networks," in *OR 2.0 Context-Aware Operating Theaters, Computer Assisted Robotic Endoscopy, Clinical Image-Based Procedures, and Skin Image Analysis*, pp. 118–127, Springer, 2018.

[107] N. Haouchine, W. Kuang, S. Cotin, and M. Yip, "Vision-based force feedback estimation for robot-assisted surgery using instrument-constrained biomechanical three-dimensional maps," *IEEE Robotics and Automation Letters*, vol. 3, no. 3, pp. 2160–2165, 2018.

[108] Y. Maeda, K. Terao, F. Shimokawa, and H. Takao, "Structural color based tactile sensor for flexible endoscopic surgery to detect grab state and organs hardness," in *2020 IEEE 33rd International Conference on Micro Electro Mechanical Systems (MEMS)*, pp. 689–692, 2020.

[109] A. Marban, V. Srinivasan, W. Samek, J. Fernández, and A. Casals, "Estimation of interaction forces in robotic surgery using a semi-supervised deep neural network model," in *2018 IEEE/RSJ International Conference on Intelligent Robots and Systems (IROS)*, pp. 761–768, 2018.

[110] E. Noohi, S. Parastegari, and M. Žefran, "Using monocular images to estimate interaction forces during minimally invasive surgery," in *2014 IEEE/RSJ International Conference on Intelligent Robots and Systems*, pp. 4297–4302, 2014.

[111] T. Watanabe, T. Iwai, Y. Fujihira, L. Wakako, H. Kagawa, and T. Yoneyama, "Force sensor attachable to thin fiberscopes/endoscopes utilizing high elasticity fabric," *Sensors*, vol. 14, no. 3, pp. 5207–5220, 2014.

[112] H. H. Ly, Y. Tanaka, and M. Fujiwara, "A tactile sensor using the acoustic reflection principle for assessing the contact force component in laparoscopic tumor localization," *International Journal of Computer Assisted Radiology and Surgery*, pp. 1–11, 2019.

[113] C. Gaudeni, L. Meli, and D. Prattichizzo, "A novel pneumatic force sensor for robot-assisted surgery," in *International Conference on Human Haptic Sensing and Touch Enabled Computer Applications*, pp. 587–599, Springer, 2018.

[114] R. S. Figliola and D. E. Beasley, *Theory and design for mechanical measurements*. John Wiley & Sons, 6th ed., 2016.

[115] P. P. Regtien and E. Dertien, *Sensors for mechatronics*. Elsevier, 2018.

[116] R. M. Schmidt, G. Schitter, and A. Rankers, *The Design of High Performance Mechatronics-: High-Tech Functionality by Multidisciplinary System Integration*. Ios Press, 2nd ed., 2014.

[117] S. Middelhoek, S. Audet, and P. French, "Silicon sensors, faculty of information technology and systems," *Delft University of Technology, Laboratory for Electronic Instrumentation, The Netherlands*, 2000.

[118] S. Yaniger, "Force sensing resistors: A review of the technology," in *Electro International, 1991*, pp. 666–668, IEEE, 1991.

[119] M. H. W. Bonse, *Capacitive Position Transducers: Theoretical Aspects and Practical Applications*. PhD thesis, TU Delft, 1995.

[120] D. Tosi and G. Perrone, *Fiber-Optic Sensors for Biomedical Applications*. Artech House, 2018.

[121] T. K. Gangopadhyay, "Prospects for fibre bragg gratings and fabry-perot interferometers in fibre-optic vibration sensing," *Sensors and Actuators A: Physical*, vol. 113, no. 1, pp. 20–38, 2004.

[122] J. Fraden, *Handbook of modern sensors: physics, designs, and applications*. Springer Science & Business Media, 5th ed., 2016.

[123] M. C. Yip, S. G. Yuen, and R. D. Howe, "A robust uniaxial force sensor for minimally invasive surgery," *IEEE transactions on biomedical engineering*, vol. 57, no. 5, pp. 1008–1011, 2010.

[124] P. Polygerinos, D. Zbyszewski, T. Schaeffter, R. Razavi, L. D. Seneviratne, and K. Althoefer, "Mri-compatible fiber-optic force sensors for catheterization procedures," *IEEE Sensors Journal*, vol. 10, no. 10, pp. 1598–1608, 2010.

[125] V. Mishra, N. Singh, U. Tiwari, and P. Kapur, "Fiber grating sensors in medicine: Current and emerging applications," *Sensors and Actuators A: Physical*, vol. 167, no. 2, pp. 279–290, 2011.

[126] A. Cusano, A. Cutolo, and M. Giordano, *Fiber Bragg Gratings Evanescent Wave Sensors: A View Back and Recent Advancements*, pp. 113–152. Berlin, Heidelberg: Springer Berlin Heidelberg, 2008.

[127] Q. Liang, K. Zou, J. Long, J. Jin, D. Zhang, G. Coppola, W. Sun, Y. Wang, and Y. Ge, "Multi-component fbg-based force sensing systems by comparison with other sensing technologies: a review," *IEEE Sensors Journal*, vol. 18, no. 18, pp. 7345–7357, 2018.

[128] D. M. Stefanescu, *Handbook of force transducers: principles and components*. Springer Science & Business Media, 2011.

[129] J. R. Brauer, *Magnetic actuators and sensors*. John Wiley & Sons, 2nd ed., 2012.

[130] K. Tadano and K. Kawashima, "Development of 4-dofs forceps with force sensing using pneumatic servo system," in *Proceedings 2006 IEEE International Conference on Robotics and Automation, 2006. ICRA 2006.*, pp. 2250–2255, IEEE, 2006.

[131] HBM, "Optical interrogators for fiber optic sensing." Accessed: 2-2-2021, from: `https://www.hbm.com/en/2322/optical-interrogators/`.

[132] P. C. Silveira, A. Dante, M. M. Keley, C. Carvalho, R. Allil, R. Mok, L. Garção, and M. Werneck, "Experimental evaluation of low-cost interrogation techniques for fbg sensors," in *2018 IEEE International Instrumentation and Measurement Technology Conference (I2MTC)*, pp. 1–6, 2018.